Annales Societatis Geologorum Poloniae (2010), vol. 80: 227–251.

STEPHANIAN–EARLY PERMIAN BASALTIC TRACHYANDESITES FROM THE SŁAWKÓW AND NIEPORAZ–BRODŁA GRABENS NEAR KRAKÓW, SOUTHERN POLAND

Anna LEWANDOWSKA[1], Mariusz J. ROSPONDEK[1], Jerzy NAWROCKI[2]

[1] *Institute of Geological Sciences, Jagiellonian University, ul. Oleandry 2a, 30-063 Kraków, Poland; e-mail: anna.lewandowska@uj.edu.pl*
[2] *Polish Geological Institute, Rakowiecka 4, 00-975 Warszawa, Poland*

Lewandowska, A., Rospondek, M. J. & Nawrocki, J., 2010. Stephanian–Early Permian basaltic trachyandesites from the Sławków and Nieporaz–Brodła grabens near Kraków, Southern Poland. *Annales Societatis Geologorum Poloniae*, 80: 227–251.

Abstract: In the Kraków–Lubliniec section of the major Hamburg–Kraków–Dobrogea Fault Zone (HKDFZ), the Stephanian–Early Permian magmatic activity was simultaneous with subsidence/uplift of the formed blocks. In the proximity of the uplifted areas the sedimentation started with fanglomerates, distally passing into playa siltstone and was accompanied by volcanism. In the Nieporaz–Brodła graben, basaltic trachyandesite a-a lava flows with autoclastic breccias reach *ca.* 150 m in thickness. The weathering recorded as adhesive rims around breccia clasts reflects palaeosoil formation during quiescence periods between the eruptions. The eruptions were effusive although scoriaceous lava indicates high volatile content of the magma. The water content before eruption had to be over 2 wt. percent. Only then the crystallisation model predicts accurately the type, composition and order of the crystallising phases. Thus, the basaltic trachyandesite magma originated from a source containing hydrous phase (*i.e.*, amphibole or phlogopite). All the studied basaltic trachyandesites had fayalitic olivine on their liquidus reflecting the crystallisation stage in a magma chamber at crustal depths. During final decompression on the magma ascent due to water exsolution, the olivine was followed by plagioclase, spinel, augite, ilmenite, apatite, K-feldspar and residual high-K rhyolitic glass. The high potassium content of these volcanics was thus a primary feature reflecting the source geochemistry and differentiation trend, and its consequence was potassium metaso- matism. Due to water exsolution the glass was altered, however, homogenous interstitial glass survived in some rocks. The glass is strongly enriched in incompatible trace elements, showing that it is a highly fractionated residual melt fraction of the basaltic trachyandesite magma. Thus, the glass geochemistry reflects the trend of fractional crystallisation indicating that co-occurring K-rich felsic rocks were not derived from the same magma.

All the basaltic trachyandesites studied have calc-alkaline to alkaline affinity. They contain fayalitic olivine and are low in MgO <5 wt. %, Cr and Ni, the features characteristic for evolved magmas. They show significant negative Sr/Sr*» 0.5–0.80 and small Eu/Eu* » 0.9–1.0 anomalies suggesting fractionation of plagioclase. The Eu/Eu* anomaly is probably compensated by amphibole retaining in the source. Negative Nb, Ti anomalies suggest Fe-Ti oxide fractionation characteristic for calc-alkaline evolution trend. A significant enrichment in LREE relatively to HREE (La/Yb ≈ 10) indicates subduction-related metasomatism. However, the described tectonic context is inconsistent with subduction-related characteristics. In conclusion, the observed geochemical characteristics indicate remarkable role of water in magma evolution. The volcanism was related to strike-slip dextral movement along the Kraków–Lubliniec section of the HKDFZ, transformed into crustal extension and subsidence, the features typical for the formation of pull-apart basins, in the late stages of the Variscan orogen evolution.

Key words: Upper Carboniferous/Permian volcanism, a-a lava flows, autoclastic breccias, basaltic trachyandesites, transitional calc-alkaline to alkaline rocks, hydrous magma.

Manuscript received 22 January 2009, accepted 1 December 2010

INTRODUCTION

Extensive Stephanian–Early Permian magmatism took place within both the Variscan orogenic belt and its foreland. In the Polish Sudetes, thick volcano-sedimentary sequences occur within the intramountain troughs: the Sub-Krkonoše Trough, the Intra-Sudetic Basin, the Żary Perycline and the North-Sudetic Basin. For example, the Intra-Sudetic Basin succession provides a record of two distinct volcanic stages: Late Carboniferous and Early Permian

post-collisional extension-related episodes (for detail discussion see: Awdankiewicz, 1999a, b; Awdankiewicz *et al.*, 2009; Awdankiewicz & Kryza, 2010a, b). Counterparts of each stage can be traced in the eastern foreland of the Variscan orogen, in the Kraków region.

The first stage of Late Carboniferous age is represented only by pyroclastic rocks intercalated with a coal-bearing terrigeneous sequence (Westphalian) of the Upper Silesian Basin (*e.g.*, Bukowy & Cebulak, 1964; Łapot, 1992). The volcanic centres have not been firmly located yet.

Volcanic rocks of the second stage mark the formation of a Stephanian–Lower Permian graben system located along the eastern margin of the Upper Silesian Coal Basin. This graben extends along a fault zone, that is the Kraków–Lubliniec Fault Zone (KLFZ) (Bogacz, 1980), which represents the contact between the Małopolska Terrane to the east and the Brunovistulian Terrane to the west (Żaba, 1995, 1999; Kalvoda *et al.*, 2008; Paszkowski *et al.*, 2007). The KLFZ is about 30 km wide section of the dextral strike-slip master dislocation: Hamburg–Kraków–Dobrogea Fault Zone (HKDFZ; Fig. 1). In this area, the Carboniferous/Permian turn yielded granodiorite intrusions (Markiewicz, 2001; Żelaźniewicz *et al.*, 2008) and extensive volcanic series (Jarmołowicz-Szulc, 1984, 1985; Harańczyk, 1989; Podemski, 2001; Nawrocki *et al.*, 2008; Słaby *et al.*, 2009). A characteristic feature of the volcanic rocks chemistry is their bimodal composition and high potassium contents (Rozen, 1909; Gaweł, 1953; Muszyński & Pieczka, 1996; Rospondek *et al.*, 2004). The rock classes, such as K-rich rhyodacites and K-rich basaltic andesites (basaltic trachyandesites) dominate (Wolska, 1984; Czerny & Muszyński, 1997), while other rock types including trachyandesites, trachytes (Muszyński, 1995) and lamprophyres are less common (Czerny & Muszyński, 1998). Previous petrographic studies of the volcanic rocks were summarised by Siedlecki (1954), and more recently by Czerny and Muszyński (1997, 1998), with the focus on geochemistry. The discussion focused on the high potassium content and genetic relationship between mafic and felsic counterparts of the volcanic series (Rozen, 1909; Bukowy & Cebulak, 1964; Czerny & Muszyński, 1997; Rospondek *et al.*, 2004; Słaby *et al.*, 2009). A close spatial relationship between both series suggests that they are genetically related. An early hypothesis on co-genetic origin of both series (Rozen, 1909) was abandoned in the course of subsequent studies (Gniazdowska, 2004; Falenty, 2004; Lewandowska & Rospondek, 2007; Słaby *et al.*, 2007, 2009). It seems likely that each series was derived from magma originated from two different sources: enriched lithospheric mantle and crust (Słaby *et al.*, 2009; Słaby *et al.*, 2010). The present study aims at discussing the issues of magma evolution, geodynamic setting and style of volcanic activity, focusing on the final stages of magma evolution of the igneous rocks of the Sławków and Nieporaz–Brodła grabens (Siedlecki, 1954; Siedlecka, 1964), using petrological data and computer modelling. In both grabens the volcanic rocks are accessible for studies from exposures and boreholes. Due to the limited number of isotope data, temporal relations between the igneous rocks are further discussed based on lithostratigraphy. Porphyritic rhyodacites occur in the form of domes and laccoliths, whereas basaltoids as both lava flows, for example at Rudno, Regulice, Alwernia and Mirów, as well as small subvolcanic intrusions, such as at Niedźwiedzia Góra (Rozen, 1909; Siedlecki, 1954), Wielkie Drogi and Zagacie. The thick basaltoid (basaltic trachyandesite) lava flows are interstratified with volcaniclastic rocks. The volcaniclastics were described by Chocyk (1989) as composed of bombs and lapilli of basaltic trachyandesites agglutinated by volcanic ash of rhyolitic composition. The difference in the clasts and matrix composition has been explained so far either as the result of the matrix siltstone formation from mixing of terrigeneous quartz-rich sediment with basaltoid material (Siedlecki & Żabiński, 1953) or as the product of simultaneous sub-aerial tephra falls of a diverse provenance (Chocyk, 1989). In the last scenario, the basaltoid bombs and lapilli would be near vent facies of basaltic trachyandesite lava eruptions, while the rhyolitic fine-grained matrix would represent distal facies of rhyolitic eruptions transported by aeolian-fluvial processes (Chocyk, 1989, 1990). In this study, these two hypotheses on the origin of the volcaniclastic rocks (Siedlecki & Żabiński, 1953; Chocyk, 1990) are discussed based on the field observations and whole-rock analyses of major and trace elements in the Sławków and Nieporaz–Brodła rock series, with reference to the composition of co-occurring rhyodacitic rocks.

GEOLOGICAL SETTING

In the Kraków region, the major W–E trending Alpine horst and graben structures are sub-parallel to the Carpathian overthrust. These include the Krzeszowice graben, the Tenczynek horst, the Rybna graben and the Carpathian Foredeep (Fig. 1). Within the Alpine horsts, the remnants of the NW–SE trending Variscan structures crop out (Bogacz, 1980); the most important of them are the Nieporaz-Brodła graben, being the southern continuation of the Sławków graben, and the adjacent Dębnik anticline (Fig. 1).

The Dębnik anticline is located along Kraków–Lubliniec Fault Zone (KLFZ), west of the mapped fault making the border with the Małopolska Terrane (Fig. 1). The anticline is penetrated by a number of intrusions, including a large rhyodacite body that intruded into the Middle Devonian carbonates forming the core of the Dębnik anticline. Its large size is evidenced by the presence of several hundred metres thick contact aureole, composed of predazzite marbles and calc-silicate rocks (Lewandowska, 1991; Rospondek *et al.*, 2009). The intrusion must have solidified relatively deep, but rapid Stephanian–Early Permian erosion of the anticline carbonates almost unroofed it, leading to its present shallow occurrence. The main body of the rhyodacite was reached by drillings at a depth of *ca.* 300 m. The sedimentary rocks of the anticline are also cut by an andesite/dacite dyke at Dubie (Muszyński & Pieczka, 1992; Lewandowska, 2009). The andesite contains porphyritic rhyodacite clasts brought up from the Dębnik rhyodacite on its way towards the surface (Harańczyk, 1989). Thus, the Dubie andesite/dacite postdates the emplacement of the Dębnik rhyodacite.

The Zalas rhyodacite was described as a laccolith (Dżułyński, 1955), and seems to be smaller or shallower than that

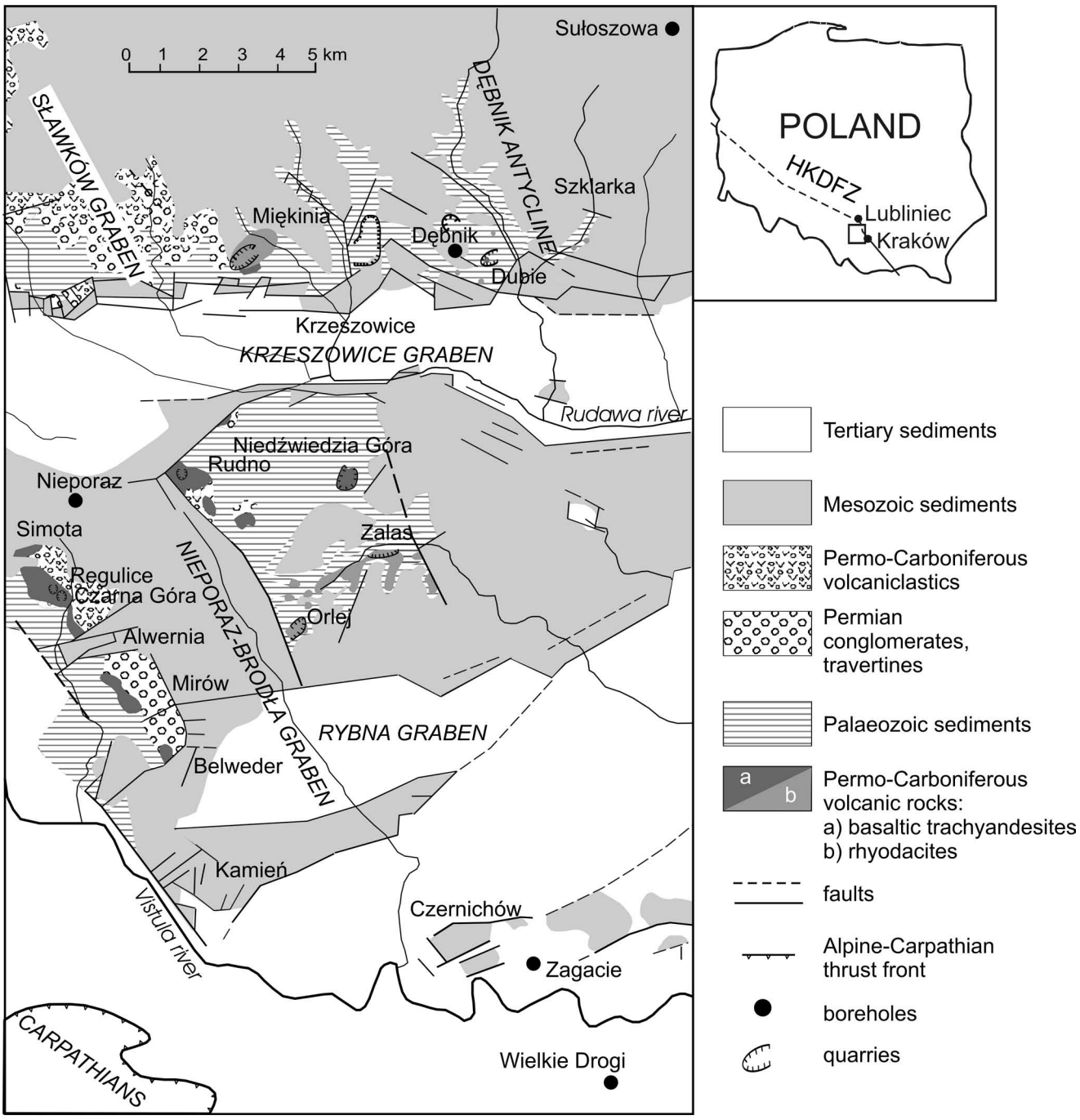

Fig. 1. Simplified geological map of the Kraków area with volcanic rock outcrops in the Sławków and Nieporaz–Brodła grabens (according to Gradziński, 1993), HKDFZ–Hamburg–Kraków–Dobrogea Fault Zone

of Dębnik, as concluded from only weak thermal metamorphism at the contact with the Lower Carboniferous siltstones and mudstones.

The uplift of the Dębnik anticline is the result of strike-slip activity of the local segment of the NW–SE trending KLFZ, that is the formation of a NNE–SSW fault system and almost perpendicular to it flat folds accompanied by the N–S and NWW–SEE flexures (Bogacz, 1980). The uplift was accompanied by a graben formation in the west, that is the Sławków graben. The sedimentary basin was filled with coarse-grained fanglomerates, representing alluvial fan deposits (Myślachowice Conglomerates). The pebbles include locally eroded limestones, dark cherts and occasionally rhyodacites (Siedlecka, 1964). The fanglomerates are overlain by the Flipowice ignimbrites (Fig. 2 Karniowice–Filipowice section). Locally, at Miękinia, a thin conglomerate bed underlies basaltic trachyandesites (Fig. 2 Miękinia section) described as a lava flow (Oberc & Parachoniak, 1962; Zajączkowski, 1972) or subvolcanic small intrusion (Czerny & Muszyński, 1997). These rocks are overlain by another fanglomerate bed followed by rhyodacite of the Miękinia dome. The Sławków graben continues beneath the Alpine Krzeszowice graben to the south as the Nieporaz–Brodła graben. Within this structure, at Zbójnik near Nieporaz

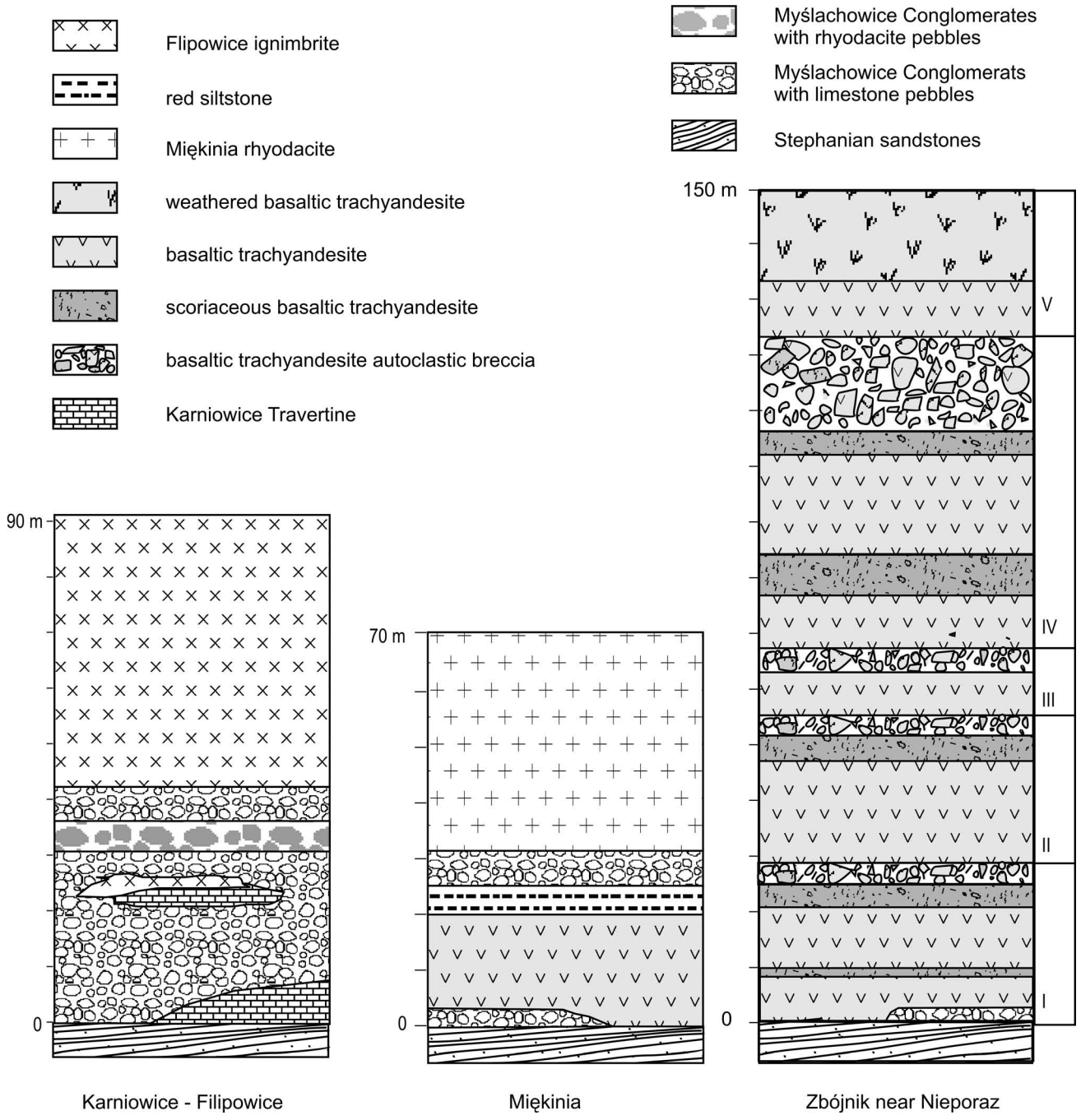

Fig. 2. Lithologic columns of the Stephanian–Early Permian succession from Karniowice–Filipowice, Miękinia and Zbójnik near Nieporaz, based on Parachoniak and Wieser (1985); Zajączkowski (1972), Roszek and Siedlecka (1966), respectively, and authors observations. Roman numbers indicate the presumed number of lava flows in the Zbójnik drill hole, according to Roszek and Siedlecka (1966)

(Fig. 2), a 150 m-thick series of basaltoid lava flows intercalates with volcaniclastic rocks and thin red sandstone beds (Roszek & Siedlecka, 1966). This volcanic sequence overlies Stephanian arkoses (Kwaczała Arkose) containing silicified araucarite stems (Birkenmajer, 1952). Locally, the volcanic rocks are also overlying and in other places intercalating with red clastic rocks, most probably forming distal fine-grained equivalent facies of the fanglomerates. The position of volcaniclastic rocks directly above the coarse-grained conglomerates suggests rapid tectonic activity, which produced conduits for magma ascents.

Initially, the Late Carboniferous age of basaltoids was suggested on the base of palaeomagnetic data (Birkenmajer, 1964) and by analogy to the other late-Variscan volcanic centres from adjacent areas (Siedlecki, 1954; Kozłowski, 1953; Bukowy & Cebulak, 1964). Later, the Early Permian age was proposed based on the Autunian fossil flora (Lipiarski, 1970) found in the Karniowice Travertine occurring as intercalations in the Myślachowice Conglomerates (Fig. 2, Karniowice–Filipowice section). The Carboniferous–Permian turn, as the age of the felsic volcanic rocks K-Ar, Ar-Ar (Jarmołowicz-Szulc, 1985; Podemski, 2001; Sko-

wroński, 1974), has recently been confirmed by the zircon SHRIMP studies of the Zalas rhyodacite indicating an age of 294.2±2.1 Ma (Nawrocki *et al.*, 2007, 2008). In turn, K-Ar dating of hornblende from the Dubie andesite also yielded a similar age, that is 291.3±6.4 Ma (Lewandowska *et al.*, 2007).

Palaeomagnetic investigations of black basaltic trachyandesites from Regulice have shown one separate NRM component, carried by magnetite, the same as noted in the greenish Zalas rhyodacites (Nawrocki *et al.*, 2008), which were dated at *ca.* 294±2.1 Ma on the base of the SHRIMP zircon age (Nawrocki *et al.*, 2007). Therefore, the felsic and basic volcanic activity seems to be almost contemporaneous what was recently confirmed by the Ar-Ar whole rock age 296.6 ± 1.5 Ma of the Niedźwiedzia Góra diabase (Nawrocki *et al.*, 2010). Latter metasomatic processes documented by adularia in the felsic volcanics (Słaby, 1990, 2000) could have been related to another magnetic component carried by hematite of the reddish basaltic trachyandesites (Nawrocki *et al.*, 2008).

The subvolcanic equivalent of the basaltoids is exposed at Niedźwiedzia Góra (Fig. 1). The Niedźwiedzia Góra basaltic trachyandesite was traditionally named diabase (*e.g.*, Gaweł, 1953; Wolska, 1984). The rock forms a sill emplaced within the Westfalian C mudstones (Bukowy & Cebulak, 1964). In the Simota Valley, at the base of the outcropped section, a massive black rock variety may represent subvolcanic rock. Other subvolcanic basaltoids were drilled within rock complexes of the southern extension of the Nieporaz–Brodła graben at Zagacie (the Zagacie-1 borehole) near Czernichów, and at Wielkie Drogi beneath the Carpathian Foredeep sedimentary infill (Fig. 1). The Wielkie Drogi basaltoid is emplaced within the Westfalian CD rocks (Łaziskie and Libiąskie beds of the Kraków Sandstone Series; Bukowy & Cebulak, 1964; Kotas, 1982), whereas the Zagacie basaltoid rests within black siltstones intercalating with coal measures and black siltstone-sandstones of the Upper Carboniferous series. It is interesting that the Zagacie and Wielkie Drogi basaltoids may occur at the southern extension of a fault bordering the Nieporaz–Brodła graben (Fig. 1). In this fault region, the Rudno outcrop of the basaltoid lava flows is presumably located. In turn, at the northern periphery of the investigated area, but outside the Nieporaz–Brodła graben, an intrusion was drilled at Sułoszowa (Fig. 1) and described by Bukowy (1975) and Harańczyk *et al.* (1995) as a gabbroid.

FIELD OBSERVATIONS

The studied basaltoids crop out in the Variscan Sławków and Nieporaz–Brodła graben system on both the northern and southern sides of the Alpine Krzeszowice graben, respectively (Fig. 1). In the north (the Sławków graben), the outcrops are limited to the Miękinia area (Heflik, 1960; Oberc & Parachoniak, 1962; Zajączkowski, 1972; Czerny & Myszyński, 1997), whereas in the south (the Niepraz–Brodła graben) they are more abundant and located along the eastern flank of the graben (Fig. 1). The best outcrops are observed in the Regulice–Alwernia area, for example in

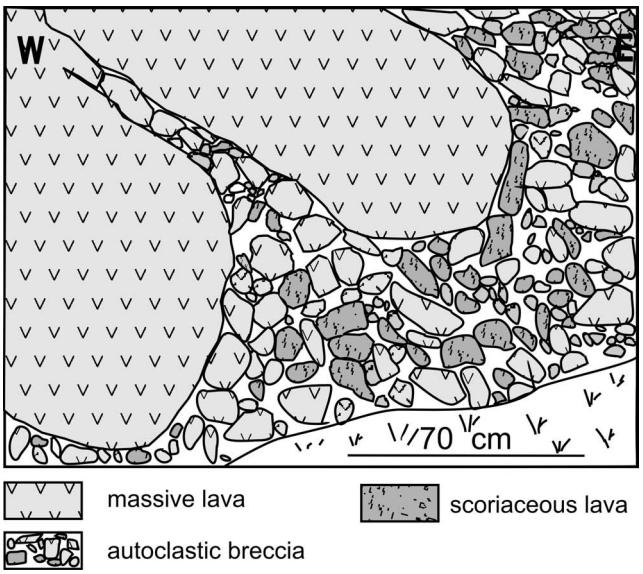

Fig. 3. Lobate lava flow fronts flanked by juvenile fragments of more scoriaceous autoclastic breccia exposed at Regulice Czarna Góra quarry

the north-western Czarna Góra quarry (fig. 7 in Lewandowska & Rospondek, 2009), where three lava flows with associated breccias are exposed. The sequence has altogether about 40 m in thickness. These basaltoid flows consist of massive central and scoriaceous top and bottom parts, often with elongated vesicles drawn out in response to the local flow direction. The lava flows often become more scoriaceous upwards with angular scoriaceous rubbles forming autoclastic breccias at the top. The passage from massive to scoriaceous lava variety is often associated with the appearance of platy structures, probably caused by streaking out of degassed vesicles. Usually, the breccias on the top are much thicker and contain more scoriaceous blocks, while those at the base are thin and composed of massive clasts. The base autoclastic breccias can be absent. In this case, the lava was solidified as blobs on uneven, weathered surface on the top of the autoclastic deposits of the previous flow (Fig. 3). The breccias are framework-supported containing massive and scoriaceous blocks, usually about 20 cm in size, but sporadically up to 50 cm large, embedded in siltstone matrix. The matrix is reddish/purple or variegated, often with horizontal lamination, suggesting gravitational filling of spaces among the blocks. The scoria is usually reddish and has vesicles up to 3 cm in size. Some vesicles are filled with secondary minerals (Żabiński, 1960; Cichoń, 1982; Parachoniak & Wieser, 1992). The sequence is comparable with a pile of three a-a lavas.

In some places (*e.g.*, separate crest rock in the SE Czarna Góra quarry; Fig 7. in Lewandowska & Rospondek, 2009), the breccias are extraordinarily thick (*ca.* 15 m) and composed of very large blocks (Fig. 4). The breccias fill a wide depression on the top of the lava flow and are composed of variable amounts of unsorted basaltoid scoriaceous clasts, up to 2–3 m in diameter, set in siltstone matrix. The presence of levees, steep deposition fronts and large angular blocks may indicate high yield strength during rock deposi-

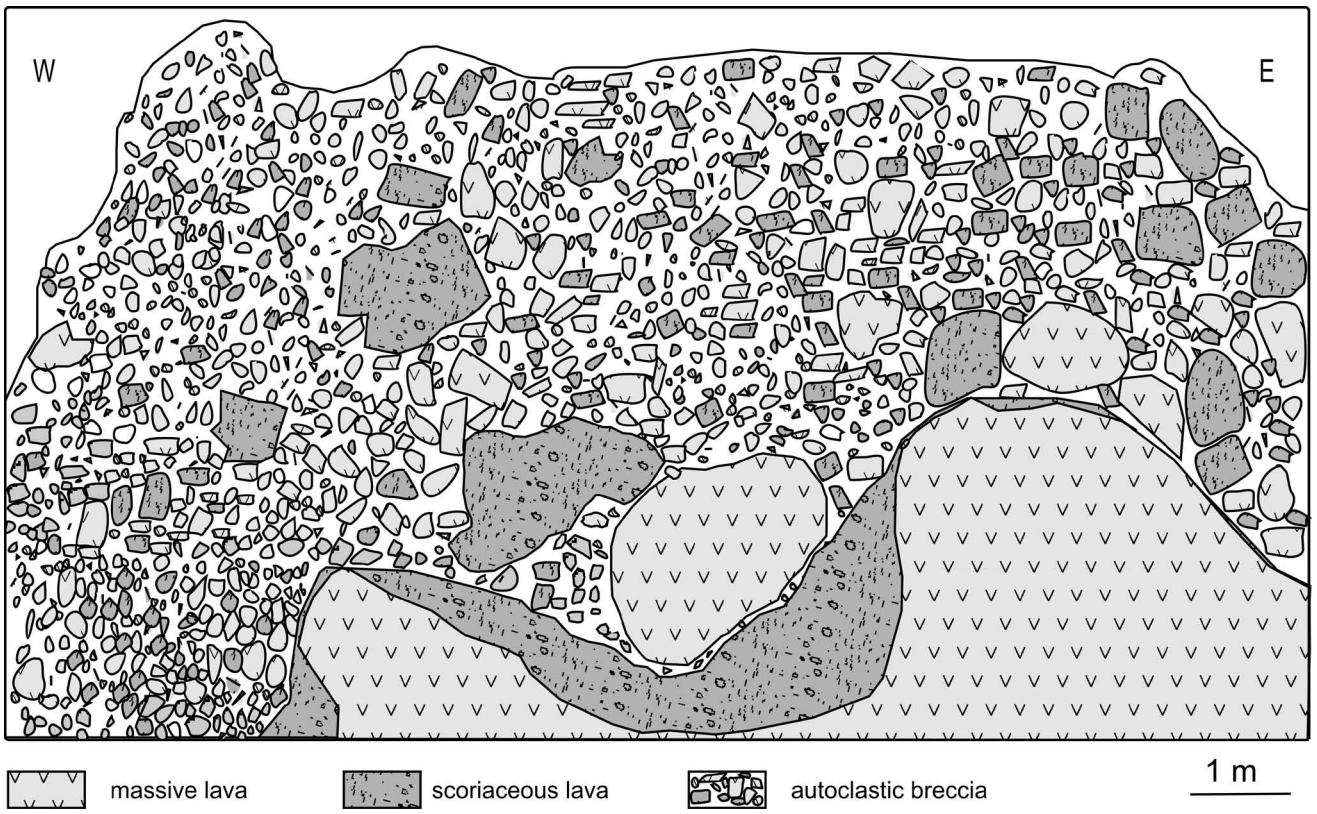

Fig. 4. A wide channel with unsorted breccias (about 6 m thick) composed of variable amount of mostly massive and scoriaceous clasts, up to several metres in diameter, interpreted as a slag heap of autoclastic breccia material accumulated at the lava front

tion. Such features are characteristic of topographically-controlled flows. The origin of this type of breccias is somewhat enigmatic. It was described as a result of scoria flow (Lewandowska & Rospondek, 2009), but alternatively could be interpreted as more distal parts of a lava flow, where brecciated material slid off the lava front or side.

The upper parts of lava flows have cracks, sometimes 0.5 m deep and 8 cm wide, filled with clastic sediments of the same type as siltstones filling structural cavities among autoclastic breccia fragments. In the sediment cognate to lavas lithoclasts, mica and quartz grains are macroscopically recognizable. The deep cracks in lava surface and the occurrence of pedogenic horizons suggest weathering episodes between subsequent lava effusions. Similar types of volcaniclastic intercalations of lavas occur also in Poręba–Mirów (Rutkowski, 1958), Rudno and in the section of the Zbójnik drillhole near Nieporaz (Fig. 2) (Roszek & Siedlecka, 1966).

SAMPLES

Samples of the volcanic rocks were collected from outcrops and boreholes. The basaltoid lava flows were sampled in the Nieporaz–Brodła graben from the outcrops at Regulice (Regulice-Czarna Góra: REG-2, REG04-1, CzG04-09, CzG-5), Simota Valley (SIM-1), Mirów (MIR-1), Rudno (RUD-1, RUD05-04, RUD05-01), Miękinia (MKW-2), and from the subvolcanic intrusion in Niedźwiedzia Góra (NG05-06, NG-1) (Fig. 1). The lavas and volcaniclastics are best exposed at the Regulice–Alwernia area, and therefore the majority of the rocks were sampled there, as well as in Rudno. The scoriaceous rock variety containing amygdales (Żabiński, 1960; Cichoń, 1982) was omitted in sampling the lavas for chemical analyses. The average amount of powdered sample was *ca.* 0.5 kg. Siltstone matrix and clasts from volcaniclastic breccias were analysed separately.

A lamprophyre sample (SzkP-1) was collected from the Pstrągarnia outcrop (Muszyński & Czerny, 1997) in the Szklarka Valley (Fig. 1).

Some of the magmatic rocks were available entirely from the drillings. These are subvolcanic equivalents of the basaltoids, which were sampled from the Wielkie Drogi borehole (Fig. 1) from the depths of 230.0 m (sample WD 230) and 476.5 m (WD476), and from the Zagacie-1 from the depth 391.7–393.8 m interval (sample ZAGAC391). The rocks are dark-green with a holocrystalline structure. The Sułoszowa sample comes from the depth of 257.8 m (sample SUL257) and was described as a gabbroid (Bukowy, 1975; Table 1 in Harańczyk *et al.*, 1995). The holocrystalline rock is patchy and consisting of greenish and reddish crystals. The gabbroid occurs close to a felsic intrusion.

METHODS

Polished thin sections were investigated using a Nikon Eclipse 600Pol petrographic optical microscope equipped with cold cathode cathodoluminescence device operating at 18 to 22 kV with current 0.4 to 0.8 mA. The modal compo-

sition of the samples investigated was integrated with the step 0.05 mm, and about 1,000 points were counted in each thin section. Moreover, scanning electron microscope (SEM) HITACHI S-4700 fitted with back scattered electron (BSE) imaging system, and coupled with a NORAN energy dispersive X-ray spectrometer (EDS) with NORAN VANTAGE analytical system at the Jagiellonian University (Poland), and wavelength-dispersive mode (WDS) on a Jeol JX 8600 at the Salzburg University (Austria) were used for qualitative and quantitative chemical analyses of minerals and interstitial glass. The WDS glass analyses were carried out on two samples from Simota. The volcanic rocks were analysed at the Keele University (England), using an ARL 8420 X-ray fluorescence spectrometer and the additional series of samples at the Salzburg University (Austria) using a Bruker-AXS, S4 Pioneer X-ray fluorescence spectrometer. Five samples were re-analysed and the results showed excellent reproducibility. The analyses were recalculated to 100 % on a volatile-free basis before plotting on the classification diagrams (Le Maitre *et al.*, 2002). The trace element contents of the interstitial glass was determined using LA-ICP-MS (laser ablation inductively coupled plasma mass spectrometry) in the Institute of Mineralogy, University of Würzburg (Germany), by a single collector quadrupole AGILENT 7500i ICP-MS, equipped with a 266 nm Merchantek LUV 266x laser. The LA-ICP-MS glass analyses were carried out on the Simota sample and the mean values are obtained for five detection points of different interstices.

RESULTS

Petrography and rock-forming minerals

Basaltic trachyandesites. The volcanic rocks from Rudno (RUD-1; RUD-2), Regulice (REG-1, REG-2, REG-3), Regulice-Czarna Góra (Cz.G. 5/2) and Mirów (MIR-1) are uniformly fine-grained, whereas the others, like Belweder (BEL-1, BEL-2), Miękinia (MKW-2) and Simota (SIM-1; Fig. 5A) represent a coarser variety (Fig. 6). The rocks are megascopically black to dark reddish, often containing a few olivine phenocrysts; thus, according to the field nomenclature by Le Maitre *et al.* (2002) the use of the name basaltoids is justified.

The fine-grained groundmass, composed of plagioclase, pyroxene, apatite and Fe-Ti oxides with few olivine phenocrysts, is a significant feature of the massive variety of basaltic trachyandesites. The phenocrysts of olivine are hyalosiderite or hortonolite containing 40–58 mol. % of forsterite and are commonly altered. The content of often idiomorphic olivine phenocrysts does not exceed 3.5 modal %, and the crystals are 0.2–3 mm in size. The olivines contain ulvöspinel-magnetite inclusions with higher Cr content compared to the others. In most lava flows, the largest plagioclase laths are 0.2–0.3 mm in size, and occasionally reach the length of 0.5 mm in subvolcanic rocks like those from Niedźwiedzia Góra (NG-10), Zagacie (ZAGAC391) and Simota (SIM-1). Normal zoning of plagioclases with labradorite core and andesine rim is most common. The plagioclases are discontinuously rimmed by potassium feldspar shells, *ca.* 0.002 mm thick. The K-feldspar rims are revealed by bright-bluish cathodoluminescence (Fig. 5B). The K-feldspar as an independent rock-forming phase is very rarely observed as tiny crystals in the interstices. Small equidimensional pyroxenes (augite) and Fe-Ti oxides are located between the plagioclase laths. Augite rarely forms twinned crystals. A series of Mg-Fe orthopyroxenes was observed in the subvolcanic rocks from Niedźwiedzia Góra only. These pyroxenes form reaction rims around augites. The Fe-Ti oxides are often represented by ulvöspinel- magnetite intergrowths with ilmenite-hematite solid solutions.

Needle-like microcrysts of apatite are set in interstices filled with glass (Fig. 5B). The interstitial glass appears as pale-grey, wedge-shaped areas (Fig. 5A). The basaltoids with abundant glass show interstitial texture (Fig. 5A). The amount of glass is in the range from 8.2 to 24.5 modal %. In the Simota (SIM-1) sample the glass is well preserved, and appears as isotropic phase. Such a pristine nature of the glass is additionally confirmed by electron microscope images revealing smooth, even surface and homogeneity of the phase filling interstices. In other samples, except for Simota (SIM-1), the glass is altered and devitrified. The altered glass appears under optical microscope as not fully transparent and inhomogeneous, stained with reddish Fe oxides. Electron microscope images show rough surfaces often with numerous platy crystals of clay minerals. In the majority of basaltic trachyandesites the alteration of interstitial glass is complementary to the breakdown of olivine. Consequently, iddingsite or bowlingite pseudomorphs after olivine are dominant in the samples containing altered glass, whereas olivine relicts survived in the Niedźwiedzia Góra and Simota (SIM-1) samples. In addition to the interstitial glass, skeletal olivine phenocrysts and apatite needles commonly represent the quench textures with hollow ends indicating rapid growth of the terminal edges.

The Zagacie and Wielkie Drogi and most of Niedźwiedzia Góra subvolcanic rocks do not contain glass. Due to the absence of glass, the textures are intergranular. In the majority of Niedźwiedzia Góra rocks, the interstices contain greenish chlorites or/and submicroscopic intergrowths of K-feldspar and quartz. The subvolcanic rock from Zagacie is similar to the one from Niedźwiedzia Góra in crystallinity as well as in the content of plagioclase and augite. Moreover, it contains chloritised hornblende but does not contain olivine and orthopyroxene. In the Zagacie sample, gabbroid xenoliths containing fresh looking olivines and pyroxenes occur. In the Wielkie Drogi sample (WD230), Fe-Ti oxides are the only opaque components.

The Sułoszowa sample (SUL257) is strongly altered, probably due to the influence of microgranite intrusion drilled in the same section (Bukowy, 1975). Alternatively, the alteration could be due to the drill hole location near the margins of a pluton, where final products of igneous crystallisation were abundant. The rock shows semi-ophitic texture with prevailing feldspars in subhedral mosaic of chloritised mafic minerals confined to the corners of feldspars (Fig. 5C). The subhedral, zoned and twinned plagioclases are andesines to albites (up to 2 mm in size) and smaller crystals of albite. The distribution of andesine to al-

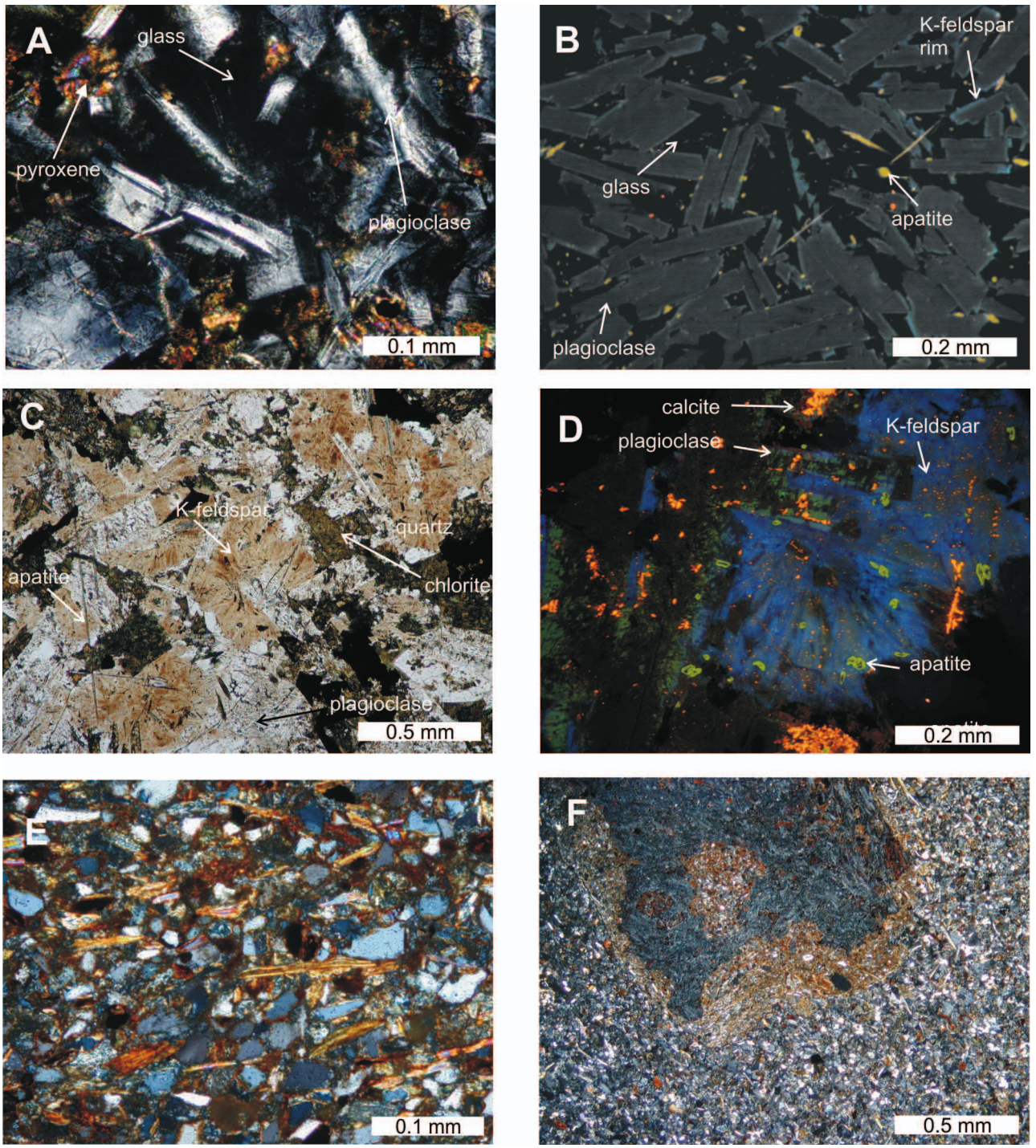

Fig. 5. Microphotographs of: (**A**) Interstitial texture with groundmass plagioclases, pyroxenes and high-K interstitial glass of basaltic trachyandesite from Simota Valley (SIM-1), crossed polars; (**B**) Plagioclases rimmed with potassium feldspar, and apatite needles in basaltic trachyandesite from Simota Valley (SIM-1), cathodoluminescence image; (**C**) Ophitic texture of the Sułoszowa quartz monzodiorite (SUL257) with dominant plagioclase overgrown by radiating (in the centre) or spherulitic (in the left corner) K-feldspars, joined as a subhedral mosaic with chloritised mafic minerals confined to the corners of feldspars, plane polarised light; (**D**) Spherulitic K-feldspars and abundant apatites in the Sułoszowa quartz monzodiorite (SUL257), cathodoluminescence image; (**E**) Tuffaceous laminated siltstone matrix of the autoclastic breccias containing feldspar and quartz fragments, including quartz shards (*e.g.*, the upper left corner), and dark and white micas from Regulice-Czarna Góra (CzG04-11), crossed polars; (**F**) A small basaltoid lithoclast with unweathered core and weathered cortex with adhesive rim (micas mimic the surface of the clast) in the autoclastic breccia from Regulice Czarna Góra (CzG04-11), plane polarised light

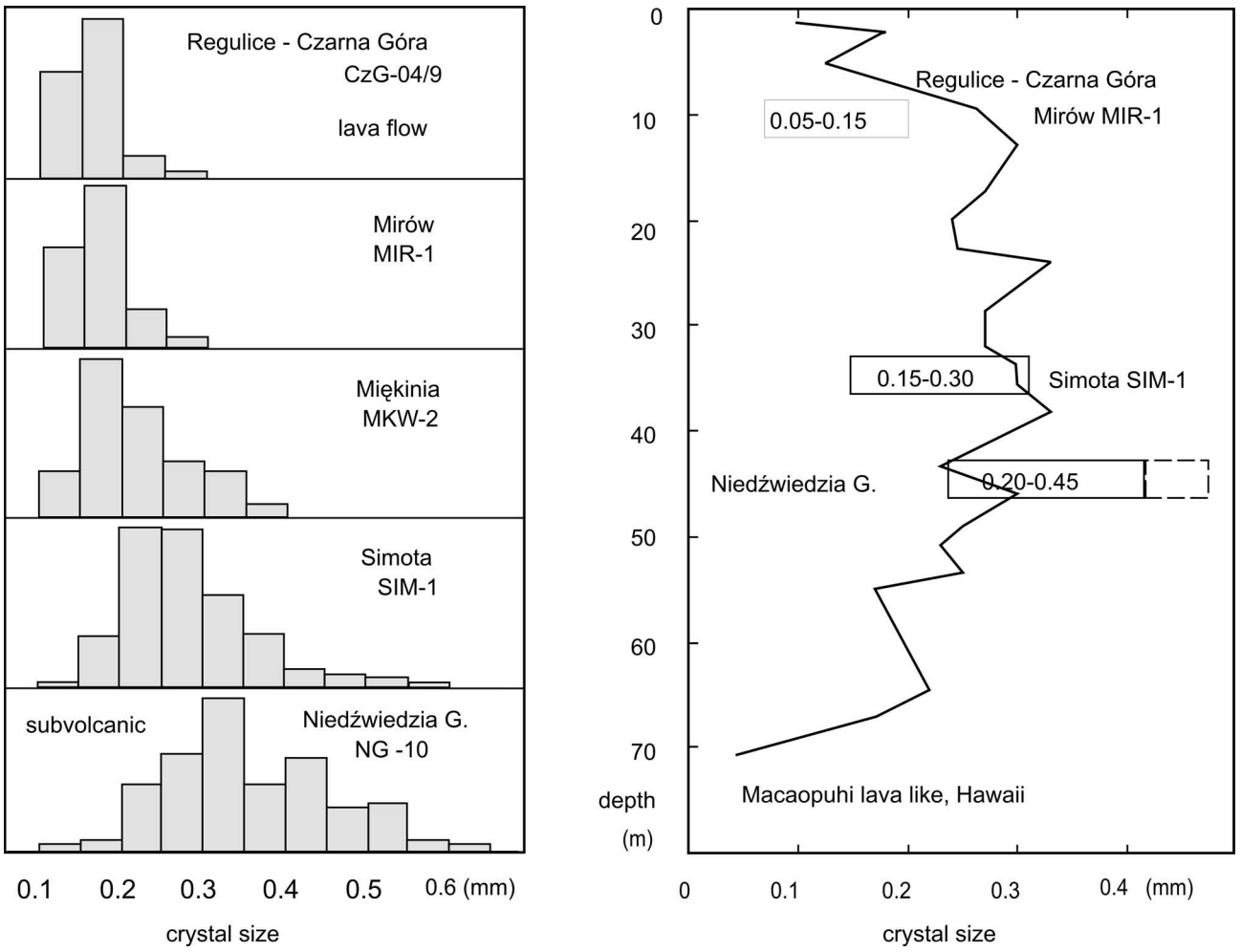

Fig. 6. Comparison of plagioclase microphenocryst sizes in the studied basaltic trachyandesites and basalt crystallised in a lava lake (Evans & Moor, 1968), roughly suggesting the crystallisation depths of basaltic trachyandesites

bite component is irregular in the crystals. The plagioclases are replaced in a patchy way by carbonates, quartz, clay minerals and K-feldspar. The K-feldspars fill the spaces between the plagioclase laths or form spherules or radiating crystals. The radiating crystals grow commonly at the faces of plagioclases that must have acted as the centres of nucleation (Fig. 5C, D). Radiating or spherulitic texture reflects an initial difficulty in crystals nucleation, followed by rapid outward growth. The K-feldspar is often reddish in plane-polarised light, presumably due to the presence of ferric iron mineral phases. Relics of unaltered amphibole are rare. There are internally incoherent pseudomorphs where a mafic phase is altered into a jumbled mass of green fibrous crystals. Pleochroic chlorites are most common products of the mafic mineral transformation. The anhedral or subeuhedral quartz is also confined to the areas between feldspars. The rock contains hollow-like apatite needles up to 1.5 mm long (Fig. 5C) and opaque minerals (0.5–1 mm in size). The presence of andesine-oligoclase (in the most calcareous plagioclase relicts), amphibole and quartz indicates that the rock was most likely quartz diorite or monzodiorite rather than gabbroid (Fig. 5C, D).

Volcaniclastic rocks. The volcaniclastic rocks, intercalating the basaltoid lava flows, represent autoclastic breccias. The breccias are framework-supported. The framework is composed of large basaltic trachyandesite blocks, whereas the fine-grained matrix is siltstone showing common horizontal lamination with normal grading (Fig. 5E). Microscopically, in the matrix there are recognisable fragments of quartz, feldspars, dark and white micas, opaque minerals, apatite and small basaltic trachyandesite lithoclasts (Fig. 5F). Quartz grains are often represented by shards and embayed crystals. The lithoclasts are commonly surrounded by a cortex composed of finer-grained fraction composed of quartz, mica and feldspar in ferrous cement (Fig. 5F), suggesting adhesive nature of the cortex (*cf.* Chocyk, 1990). It is clear that the fragmentation of some minerals was pyroclastic as evidenced by shards (Fig. 5E). They are juvenile and have not been reworked much by epiclastic superficial processes. The fragments of K-feldspar crystals show blue cathodoluminescence, while less frequent plagioclase fragments are greenish. The biotite flakes are common (from 8 to 18 modal %). The grains are embedded in clay matrix.

Geochemistry

Whole-rock geochemistry. The bulk rock major and trace element content is given in Table 1. All the basaltoids of the Nieporaz–Brodła graben, including the subvolcanic equivalents, have a relatively narrow range of silica content from 51 to 56 wt. % SiO_2 (Table 1). Such a composition and high alkali content locate them in the basaltic trachyandesite S2 field on the TAS classification diagram (Fig. 7A). The data are scattered around the line separating the fields of calc-alkaline and alkaline rocks (transitional series). Such characteristics also hold for diabases from Zagacie (ZGAC 391), Wielkie Drogi (WD 230), and Sułoszowa samples (SUL257), which have been analysed for the first time. Several samples showing higher alkali content, namely basaltoids from the upper part of the lava flows at Czarna Góra (Chocyk, 1989) and scoriaceous blocks from autoclastic breccias, plot in the phonotephrite field (Fig. 7A). A similar position of the second (WD476) of the Wielkie Drogi samples (Table 1) results from its hydrothermal alteration.

On the other hand, on the SiO_2-K_2O classification diagram the analysed rocks plot in the high-K basaltic andesite field, while several analyses of Niedźwiedzia Góra plot along the border with high-K basalt field (Fig. 7B). The appropriately high K/Na ratios classify some of them as shoshonites (Le Maitre *et al.*, 2002). The rocks form an uniform group and the differences are due rather to the nature of both classifications ($Na_2O + K_2O$ and K_2O), in which the field separating lines are differently designed. The whole-rock analysis from Czerny and Muszyński (1997) and Chocyk (1989) are included in Fig. 7.

On the discussed classification diagrams, the SiO_2 and alkali content of the tuffaceous siltstone matrix of the breccias (Table 1) locates the siltstones in the rhyolite field (Fig. 7A). The SiO_2 is usually in the range from 74 to 77 wt. %. Significantly lower SiO_2 content from 64 to 69 wt. % are found in two samples containing abundant basaltic andesite lithoclasts. Such high K_2O contents are in the range of those found in the Zalas, Miękinia and Dębnik rhyodacites and in the residual interstitial glass of the basaltic trachyandesites (Fig. 7B). The Filipowice ignimbrites fall in the trachyte/trachyandesite field, but are out of the classification fields in the SiO_2/K_2O diagram due to too high potassium content.

The lamprophyres data scatter all over the chemical classification diagrams due to secondary alterations (Czerny & Muszyński, 1998). The least altered sample (SzkP-1) from Szklarka plots in the fields of trachyte/dacite (Fig. 7A), but the high K_2O content locates these samples out of the classification fields (Fig. 7B). All the rocks showing features of metasomatic alteration are omitted in further discussions on their trace element geochemistry. The most altered samples are lamprophyres and the Sułoszowa quartz monzodiorite.

Interstitial glass geochemistry. The glass is altered in all but one sample of the basaltic trachyandesite. The Simota (SIM-1) sample is exceptional, since its glass domains show no symptoms of alteration. The glass composition is fairly homogenous, and it is microscopically isotropic. The glass consists of network-forming elements, like SiO_2 (74.6–77.5 wt. %) and Al_2O_3 (12.3– 13.4 wt. %), with other elements ranging as follows: K_2O (3.8–4.9 wt. %), Na_2O (2.2–3.3 wt. %), FeO_T (1.2–2.0 wt. %), CaO (0.3–1.9 wt. %), MgO (0–0.3 wt. %), TiO_2 (1.4– 2.0 wt. %), Cl (0.1–0.2 wt. %), P_2O_5 (0.1–0.5 wt. %), and MnO (0–0.2 wt. %) on the volatile-free basis (Table 2). The WDS analyses showed analytical totals implying the H_2O content of 4–7 wt. %. The interstitial glass composition plotted on the TAS classification diagram (Fig. 7A) revealed its rhyolitic composition and again the K_2O content is high enough to plot it in the high-K rhyolite field (Fig. 7B). The incompatible ele-

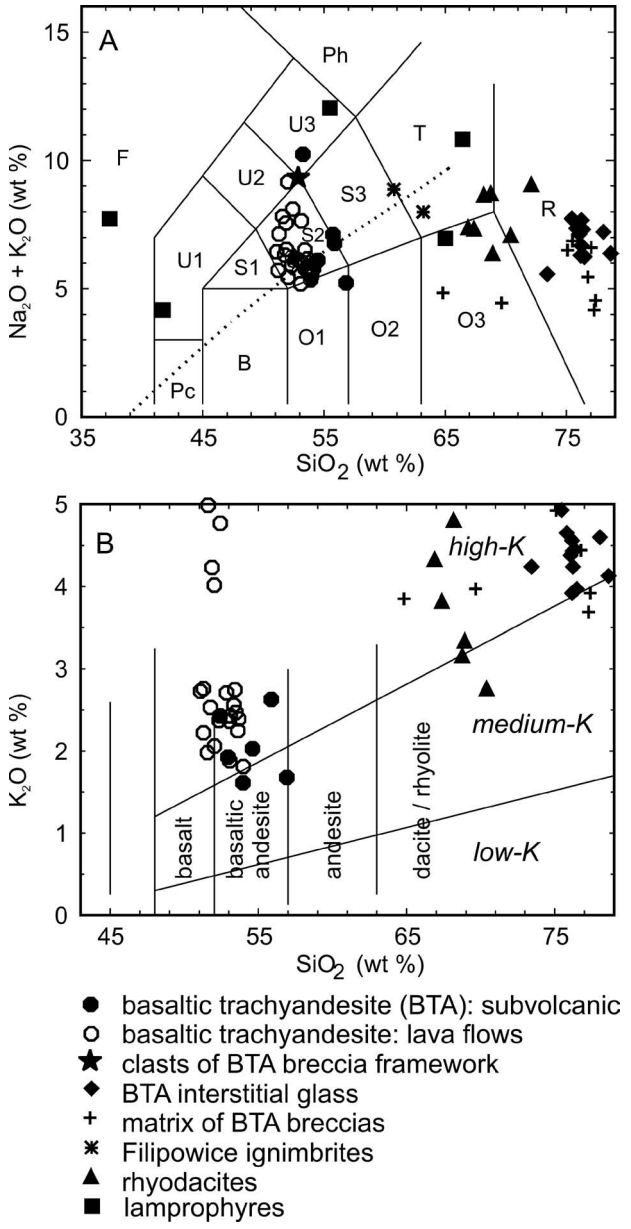

Fig. 7. The comparison of chemistry of volcanics from the Nieporaz–Brodła graben: on the (A) TAS and (B) K_2O-SiO_2 classification diagrams (Le Maitre *et al.*, 2002). Rock analyses by Czerny and Muszyński (1997, 1998) and Chocyk (1989) are included; Pc – picrobasalt, B – basalt, O_1 – basaltic andesite, O_2 – andesite, O_3 – dacite, S_1 – trachybasalt, S_2 – basaltic trachyandesite, S_3 – trachyandesite, T – trachyte/trachydacite, R – rhyolite, F – foidite, U_1 – tephrite/basanite, U_2 – phonotephrite, U_3 – tephriphonolite, Ph – phonolite

Table 1

Geochemistry of the investigated samples

Sample name	REG-2	REG04-1	CzG 04-09	CzG-5	MIR-1	RUD-1	RUD 05-04	RUD 05-01	MKW-1	SIM-1	NG05-06	NG-1
Locality	Regulice				Mirów	Rudno			Miękinia	Simota	Niedźwiedzia Góra	
Rock type	basaltic trachyandesite lava flows								diabase?		diabase	
SiO_2	53.94	51.88	53.07	52.04	52.41	53.66	51.09	51.60	53.98	53.87	52.94	54.13
TiO_2	1.60	1.67	1.54	1.55	1.71	1.71	1.69	1.65	1.76	1.78	1.74	1.79
Al_2O_3	16.73	17.24	15.77	16.05	17.05	16.53	16.16	15.94	16.12	16.07	15.32	16.09
Fe_2O_3*	8.45*	8.97*	8.71*	8.54*	10.38*	9.76*	10.24*	10.97*	9.98*	10.49*	10.68*	10.52*
MnO	0.120	0.08	0.14	0.10	0.090	0.140	0.14	0.08	0.120	0.170	0.16	0.170
MgO	4.96	3.81	4.62	4.80	3.23	3.71	4.28	3.36	3.00	3.70	3.66	3.83
CaO	7.43	6.82	7.32	7.57	4.15	6.70	5.98	4.03	6.82	6.89	6.43	6.53
Na_2O	3.45	3.69	3.31	3.38	3.33	3.78	3.71	2.83	3.80	3.73	3.72	3.83
K_2O	2.04	2.84	1.88	2.06	4.77	2.39	2.73	4.99	1.81	1.62	1.93	1.97
P_2O_5	0.47	0.35	0.41	0.40	0.72	0.70	0.62	0.63	0.87	0.83	0.75	0.88
LOI	1.11	2.66	2.41	2.99	1.77	0.99	4.34	4.43	1.34	1.19	1.32	0.67
Total	100.3	100.01	99.18	99.48	99.61	100.07	100.98	100.51	99.6	100.34	98.65	100.41
Cr	125	148	124	137	97	76	87	103	63	71	69	74
Ni	79	77	73	84	57	50	52	49	47	48	45	46
Co	n.a.	27	25	24	n.a.	n.a.	23	21	n.a.	n.a.	22	n.a.
Sc	n.a.	21	18	19	n.a.	n.a.	21	22	n.a.	n.a.	18	n.a.
V	170	166	174	166	203	136	154	210	121	130	124	118
Cu	34	n.a.	n.a.	n.a.	33	36	n.a.	n.a.	48	49	n.a.	47
Pb	17	19	14	16	20	19	13	22	17	15	15	17
Zn	80	82	92	79	143	110	113	105	135	105	117	120
S	59	n.a.	n.a.	n.a.	53	53	n.a.	n.a.	68	51	n.a.	83
Rb	29	49	44	27	72	50	43	77	49	53	33	44
Ba	1,007	905	955	955	1,134	1,020	832	931	920	881	666	748
Sr	876	841	862	901	789	822	734	521	468	556	429	495
Ga	19	20	18	18	24	22	20	19	20	22	21	22
Nb	18	14	14	17	27	28	23	25	39	35	33	38
U	n.a.	n.a.	n.a.	2	n.a.	n.a.	n.a.	n.a.	n.a.	1	1	1
Ta	n.a.	n.a.	n.a.	1	n.a.	n.a.	n.a.	n.a.	n.a.	2	2	2
Zr	240	246	237	229	309	312	292	309	414	365	375	386
Y	34	24	31	29	39	42	39	35	53	48	47	51
Th	8	11	9	11	9	6	8	8	3	5	4	4
La	55	57	60	60	83	64	67	61	61	64	59	55
Ce	133	113	126	137	175	138	150	147	134	122	141	121
Pr	n.a.	n.a.	n.a.	14	n.a.	n.a.	n.a.	n.a.	n.a.	15	15	15
Nd	55	54	67	66	57	53	64	65	54	55	54	50
Sm	n.a.	n.a.	n.a.	9	n.a.	n.a.	n.a.	n.a.	n.a.	10	10	11
Eu	n.a.	n.a.	n.a.	2	n.a.	n.a.	n.a.	n.a.	n.a.	3	3	3
Gd	n.a.	7	10	10	n.a.	n.a.	12	10	n.a.	9.48	11	n.a.
Dy	n.a.	4	5	5	n.a.	n.a.	6	5	n.a.	n.a.	7	n.a.
Yb	n.a.	2	2	2	n.a.	n.a.	3	3	n.a.	n.a.	4	n.a.
Cl	41	556	279	79	52	54	113	228	191	154	128	107

n.a.– not analysed, n.d. – not detected, Fe_2O_3* – total iron

Table 1 continued

Sample name	WD230	WD476	ZAGAC 391	SUL257	REG 04-1a	RUD 05-2	RUD 05-03	REG 04-1b	CzG 04-10	CzG 04-11	CzG 04-N4	ZAL-922	SzkP-1
Locality	Wielkie Drogi		Zagacie	Sułoszowa	Regulice	Rudno	Rudno	Regulice	Czarna Góra			Zalas	Szklarka P.
Rock type	diabase			quartz monzodiorite	volcaniclastic clasts		volcniclastic matrix					rhyodacite	lamprophyre
SiO_2	55.83	53.24	55.72	53.40	53.26	52.89	63.82	73.56	76.28	77.40	69.66	70.60	55.48
TiO_2	1.48	1.56	1.45	2.31	1.76	1.72	0.51	0.49	0.42	0.44	0.55	0.38	0.76
Al_2O_3	16.29	16.15	16.10	13.14	15.15	14.98	12.30	10.69	9.39	8.45	10.85	14.96	14.61
Fe_2O_3*	7.48*	8.21*	7.14*	13.23*	10.38*	11.17*	4.55*	3.83*	2.93*	1.63*	5.95*	3.03*	5.13*
MnO	0.05	0.109	0.10	0.177	0.07	0.07	0.07	0.07	0.05	0.05	0.10	0.030	0.05
MgO	4.25	4.11	4.26	3.97	2.07	2.88	5.47	1.87	4.28	1.76	3.13	0.72	1.08
CaO	5.05	3.18	5.09	2.86	2.94	2.47	0.59	0.81	0.4	2.12	0.49	2.13	9.49
Na_2O	4.19	1.26	4.61	3.76	2.22	1.51	0.99	1.22	0.48	0.62	0.47	3.36	0.80
K_2O	2.62	8.97	2.50	2.75	7.21	7.95	3.85	3.58	3.69	3.92	3.97	3.19	11.25
P_2O_5	0.44	0.40	0.42	0.37	0.59	0.67	0.08	0.07	0.10	0.07	0.08	0.09	0.59
LOI	2.26	0.70	1.45	0.81	4.73	4.61	9.47	4.35	4.20	3.90	4.64	1.39	0.35
Total	99.94	97.89	98.84	96.78	100.38	100.92	101.7	100.54	102.22	100.36	99.89	99.88	99.59
Cr	91	130	96	20	123	96	63	119	54	62	68	16	91
Ni	59	62	61	5	51	48	66	63	61	49	70	6	68
Co	16	20	20	28	21	13	17	17	13	9	15	n.a.	14
Sc	14	17	13	32	23	17	7	8	9	7	8	n.a.	14
V	150	187	149	237	188	135	62	75	69	60	86	41	221
Cu	n.a.	25	n.a.	16	n.a.	n.a.	n.a.	n.a.	n.a.	n.a.	n.a.	5	58
Pb	11	8	13	7	17	19	9	10	5	4	17	20	15
Zn	100	34	76	107	86	103	124	87	53	48	87	41	104
S	n.a.	n.a.	n.a.	n.a.	n.a.	n.a.	n.a.	n.a.	n.a.	n.a.	n.a.	66	n.a.
Rb	50	95	49	58	89	101	103	111	86	85	149	103	157
Ba	908	720	1,089	387	1,037	925	303	289	252	245	297	868	548
Sr	741	35	757	217	449	273	75	81	46	47	43	217	137
Ga	17	17	20	23	19	19	23	17	13	10	16	17	20
Nb	13	15	14	18	21	25	12	9	10	8	11	8	10
U	1	n.a.	1	n.a.	n.a.	n.a.	n.a.	n.a.	n.a.	n.a.	n.a.	n.a.	n.a.
Ta	1	n.a.	1	n.a.	n.a.	n.a.	n.a.	n.a.	n.a.	n.a.	n.a.	n.a.	1
Zr	216	178	202	254	308	309	158	161	116	186	138	136	298
Y	24	20	25	48	37	40	17	18	15	17	17	13	14
Th	4	10	5	5	18	7	10	6	4	5	9	2	31
La	51	38	52	24	85	68	19	24	12	10	21	16	93
Ce	104	75	93	58	204	153	28	27	15	9	33	39	161
Pr	13	n.a.	13	n.a.	n.a.	n.a.	n.a.	n.a.	n.a.	n.a.	n.a.	n.a.	n.a.
Nd	56	50	53	38	86	79	8	11	8	6	19	22	104
Sm	8	n.a.	8	n.a.	n.a.	n.a.	n.a.	n.a.	n.a.	n.a.	n.a.	n.a.	n.a.
Eu	2	n.a.	2	n.a.	n.a.	n.a.	n.a.	n.a.	n.a.	n.a.	n.a.	n.a.	n.a.
Gd	6	n.a.	7	n.a.	12	9	2	4	n.d.	1	n.d.	n.a.	n.a.
Dy	3	n.a.	4	n.a.	6	6	3	2	2	2	3	n.a.	n.a.
Yb	2	n.a.	2	n.a.	3	3	1	2	2	1	1	n.a.	n.a.
Cl	278	953	181	199	524	263	304	84	88	77	98	21	206

n.a.– not analysed, n.d. – not detected, Fe_2O_3* – total iron

Table 2

Representative point analyses of the interstitial glass from the Simota Valley (SIM-1)

Analytical point	SiO_2	TiO_2	Al_2O_3	Fe_2O_3*	MnO	MgO	CaO	Na_2O	K_2O	P_2O_5	Cl
EDS											
1	76.05	1.79	12.74	1.24	0.06	0.14	1.33	2.33	3.94	0.25	0.13
1a	75.06	1.62	13.37	1.19	0.02	0.26	1.93	2.35	3.85	0.29	0.06
2	75.50	1.68	12.53	1.98	bdl	0.05	0.45	2.71	4.63	0.31	0.15
2a	75.80	1.57	12.72	1.67	0.1	0.17	0.41	3.08	4.12	0.25	0.1
3	75.53	1.95	12.49	1.45	bdl	0.18	0.41	3.29	4.28	0.26	0.16
3a	77.47	1.65	12.40	1.3	0.08	0.18	0.34	2.44	3.76	0.26	0.13
3b	76.77	1.91	12.37	1.24	0.07	0.01	0.38	2.15	4.62	0.30	0.17
10	75.45	1.65	12.73	1.62	bdl	0.20	0.42	2.89	4.54	0.32	0.19
14	74.61	1.76	13.39	1.29	bdl	0.16	0.53	2.85	4.88	0.35	0.18
11	75.36	1.46	12.71	1.6	0.15	0.32	1.11	2.62	4.17	0.37	0.13
12	75.63	1.46	12.87	1.54	0.19	0.12	0.27	2.88	4.39	0.53	0.13
13	77.26	1.39	12.31	1.42	0.03	0.07	0.69	2.49	4.10	0.08	0.15
WDS											
a	72.75	1.58	13.68	0.52	bdl	0.03	0.37	1.70	4.53	bdl	0.27
b	73.33	1.73	13.21	0.65	bdl	bdl	0.26	1.24	4.14	bdl	0.18

bdl – below detection limit, Fe_2O_3* – total iron

ment content is Zr 1149 ppm and Y 119 ppm, while the compatible that of Cr, Co, Ni is 1, 4, and 6 ppm, respectively. The attempts at analysing devitrified glass of other samples gave scattered results. For example, in Belweder sample (BEL-1) devitrification led to significant enrichment in SiO_2 to 92 wt. % and depletion in all other elements.

DISCUSSION

Volcanic rocks have recorded the information on their evolution. Their components, structures and textures can reveal their source (*e.g.*, from xenoliths), but usually are able to track their evolution from the beginning of the crystallisation to solidification. The type of volcanic edifices, lava flows, and the relationship within volcano-sedimentary sequences can shed light on its eruptive history. Their geochemistry often allows one to formulate hypotheses on geotectonic setting of parental magma generation. The following sections are planned to discuss these issues.

Evolution of magma

The basaltic trachyandesites from the Kraków area contain neither xenoliths nor xenocrysts. The crystals of olivines have fairly too fayalitic (Fo_{40-58}) composition to represent mantle xenocrysts. The olivine of $Fo_{88–92}$, would be a good candidate for a mantle source (Carmichael, 2002). Moreover, the olivine crystals have frequently skeletal forms, clearly indicating their origin from quickly quenching magma. Thus, the rock mineral assemblage bears clear evidence of magmatic origin. The first record of the magma evolution comes from the fayalitic olivine phenocrysts containing rare Cr-ulvöspinel and ubiquitous ilmenite inclusions. The co-crystallisation of ilmenite with fayalitic olivine would mark the crystallisation from silica-saturated melt or less likely the equilibration of the melt with silica-saturated rocks in the source (Frost *et al.*, 1988; Lange & Carmichael, 1996).

Diversity of crystal sizes in volcanic rocks reveals that different crystal-size populations formed under varying conditions, that is particularly at different temperatures and pressures. The investigated rocks contain small amounts of phenocrysts, abundant microphenocrysts of the groundmass, and tiny crystals and glass in the interstices (Rospondek *et al.*, 2004). Such a structure suggests the evolution of the rock in three stages (Lewandowska *et al.*, 2008). The first stage presumably represents slow cooling in a magma chamber prior to magma ascent, the second rapid decompression and concurrent cooling on ascent and eruption, while the last one – post-eruptive cooling. Consequently, a model of three stages of the evolution of crystal-liquid system was verified for the Simota SIM-1 basaltic trachy-an desite composition at $f_{O2} \leq$ MH (magnetite-hematite) buffer using the MELTS program (Ghiorso & Sack, 1995). Such an oxygen fugacity value was tentatively assumed basing on the presence of Fe-Ti oxides and Ca-rich augite. The program predicts at each stage the composition and proportion of liquid and solid phases that are stable at each increment of cooling or decompression for melt compositions, ranging from potassium ankaratrites to rhyolites, over the temperature range 900°–1700° C and pressures up to 40 kbar. The type of mineral assemblage and texture of the basaltic trachyandesites can be modelled only when assuming significant initial water content in the melt (Lewandowska *et al.*, 2008). “Several studies of experimental phase equilibria

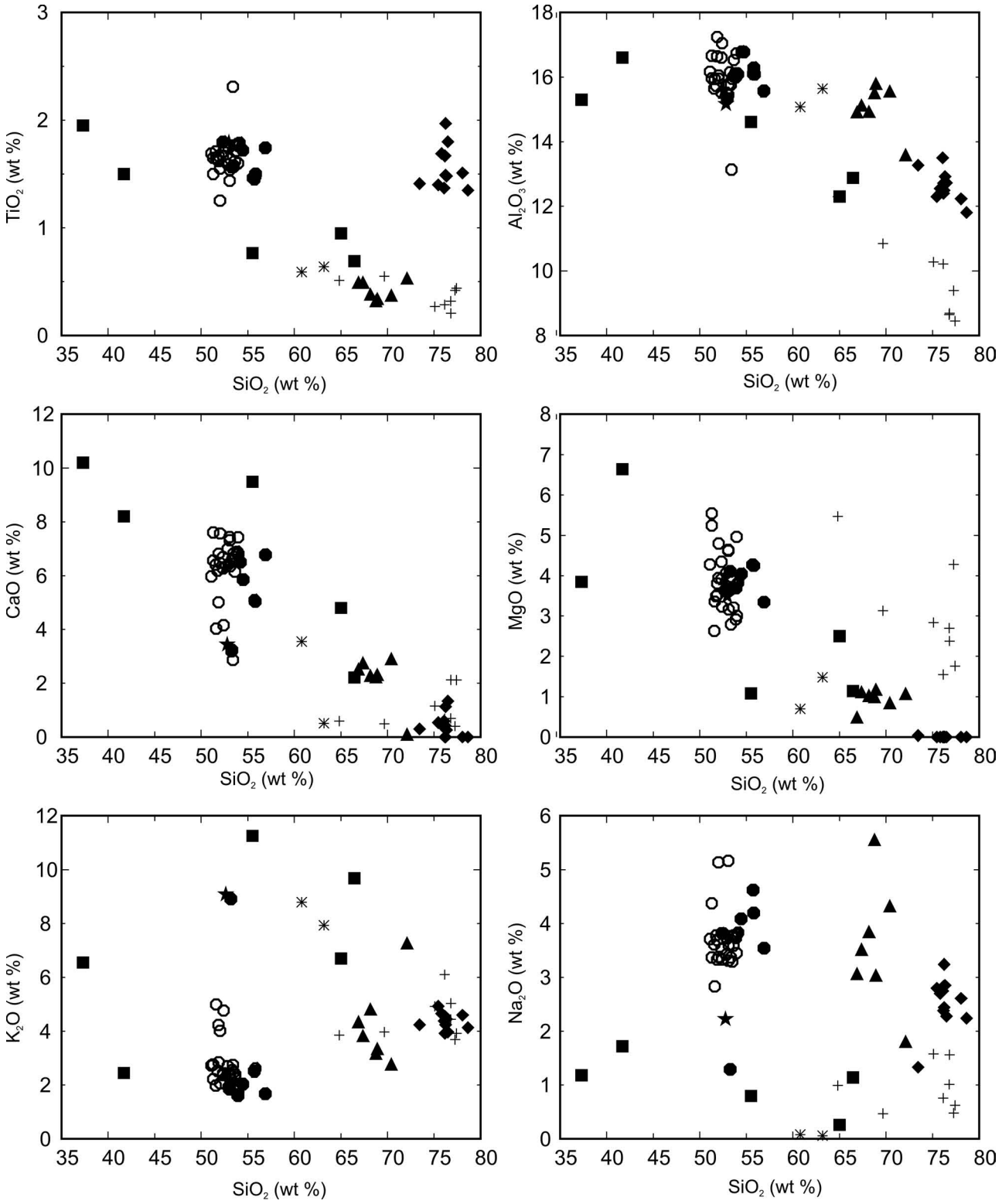

Fig. 8. Harker-type diagrams showing compositional variations of the volcanics from the Nieporaz–Brodła graben, rock analyses by Czerny and Muszyński (1997, 1998) and Chocyk (1989) are included, symbols like in Fig. 7

on such lavas relate water concentration to the phenocryst assemblages and to the degree of crystallinity, so that the abundance, composition and variety of phenocrysts can be used to constrain the amount of water dissolved in the magma" (Carmichael, 2002, p. 641). The experiments have come along with the MELTS simulations (Ghiorso & Sack, 1995). Only when magma contains over 2 wt. % of water, olivine does start to crystallize first at *ca.* 1080°C and moderate pressure 1–2 kbar and it is joined by spinel and plagioclase at somewhat lower temperatures. The liquidus temperature is similar to that found for other compositional variety of basaltic andesites (Sission & Grove, 1993). The

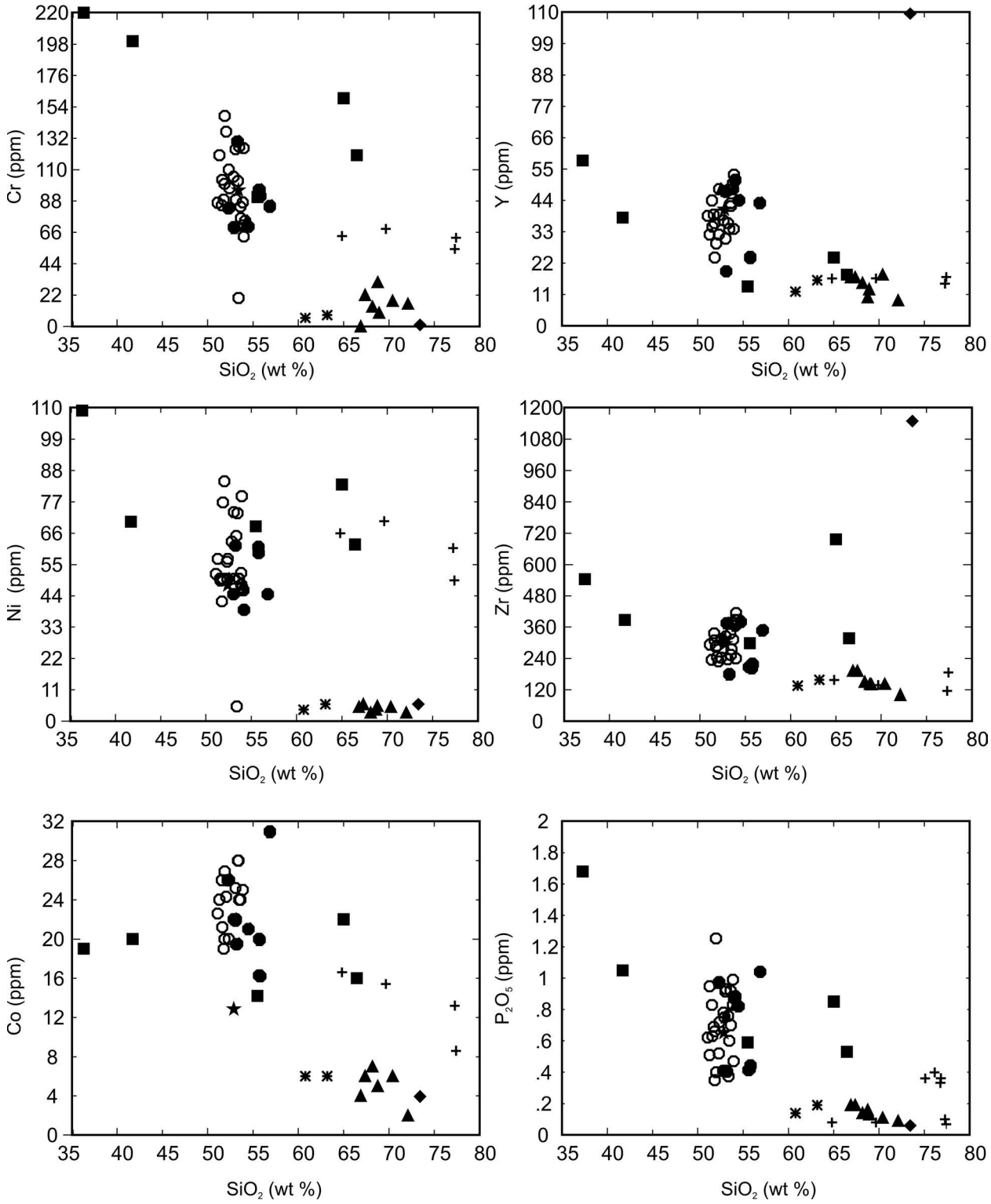

Fig. 8 continued

nucleation of plagioclase starts before water exsolution because only significant water content stabilizes the $CaAl_2Si_2O_8$ component of plagioclase (Housh & Luhr, 1991; Moore & Carmichael, 1998). Thus, the observed labradorite core of microphenocrysts could be explained only by assuming a period of crystallisation at a relatively higher water pressure (>1 kbar). Such pressures occur in the upper crust, where most magmas including basaltic trachyandesitic ones appear to reside prior to eruptions (Luhr, 1990; Rutherford *et al.*, 1985; Rutherford & Devine, 1988; Sission & Grove, 1993). The second stage is characterised by decompression resulting in rapid plagioclase and clinopyroxene crystallisation (Fig. 5A, B) due to water exsolution, presumably during magma ascent and eruption. The

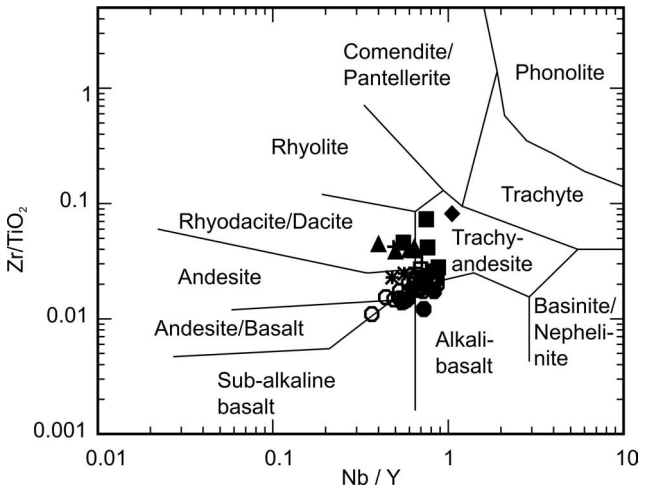

Fig. 9. The comparison of chemistry of the volcanics from the Nieporaz–Brodła graben on the Nb/Y– Zr/TiO_2 discrimination diagram (Winchester & Floyd, 1977); rock analyses by Czerny and Muszyński (1997, 1998) and Chocyk (1989) are also included, symbols like in Fig. 7

water is mostly lost to the conduit or to the rocks surrounding it, and its small fraction also reacts with the olivine to form iddingsite at oxidizing conditions (*e.g.*, Furgal & McMillan, 2001). The iddingsite formation, however, cannot be verified by the modelling due to the lack of the thermodynamic data. At this stage, the magma crystallinity reaches the eruptibility limit of *ca.* 50% (*e.g.*, Carmichael, 2002). At the final low-pressure and low-temperature stage the plagioclase continues to grow. The plagioclase rims become composed of K-feldspar, which also rarely forms separate tiny crystals in the interstices (Fig. 5A, B). This observation is consistent with finding of such rims in recent shoshonites (*e.g.*, Nicholls & Carmichael, 1969) and indicates that the K-feldspar is a primary magmatic phase. Other crystallising minerals are needle-like apatite, rhm-oxides (ilmenite) and spinel. Several percent of the remaining melt reaches high-K-rhyolitic composition and is quenched to glass in the interstices. Only in subvolcanic rocks from Niedźwiedzia Góra, the crystallisation advances further on, leading to quartz formation in the interstices. The partial re-equilibration at very shallow depths results in the formation of the orthopyroxene coronas around augites. Orthopyroxenes are not observed in the rapidly quenched lava flows. For basaltic trachyandesite magmas the orthopyroxene is stable at low pressure only. On the other hand, the high pressure crystallisation may be recorded in the Zagacie sample by the assemblage containing hornblende, which is not stable below *ca.* 1 kbar reflecting primary water content of *ca.* 4.0 wt. % (*e.g.*, Carmichael, 2002). All these suggest that the magmas were generated from a source containing a hydrous phase component (*i.e.*, phlogopite or amphibole). In fact, partial melting of amphibolite can produce melt of the andesitic and basaltic andesite composition (Carmichael, 2002).

The compatibility of the modelled mineral assemblages and the basaltic trachyandesite mineral composition (for modal composition see Table 1 in Rospondek *et al.*, 2004) shows that the proposed scenario describes well the formation of these rocks in nature from the liquidus stage in a magma chamber, through magma ascent, up to the solidification at the surface. The proposed evolution also attests that the potassium metasomatism is a consequence of the water exsolution simultaneous with residual melt enrichment in potassium.

Type of volcanic activity

In the Nieporaz–Brodła graben, three outcropping basaltic trachyandesite lava flows contain volcaniclastic intercalations, mainly framework-supported breccias with red siltstone matrix. The same type of siltstone also fills fissure reaching down into the underlying lava flows. The nature of these volcaniclastic rocks was not clear.

Some volcaniclastic breccias were interpreted by Chocyk (1990) as a result of sub-aerial fall out tephra: lapillites and agglomerates, although in the course of our field studies such rocks were not found. The observed breccias contain angular, both massive and scoriaceous rubbles and no evidence of ballistic bombs impacts was recorded in the laminated fine-grained sediments. Spindle bombs were not found either. Instead, the geochemical and petrographic similarity of the blocks in the breccias to the underlying basaltic trachyandesite flows suggests that the rocks are autoclastic breccias associated with a-a lava flows.

The siltstones have high-K rhyolitic composition (Fig. 7B) and contain an admixture of pyromorphic mineral clasts in clay matrix (Fig. 5E). The clay fraction consists of mixed-layered illite/smectite minerals, which were formed from devitrification of felsic volcanic glass (Chocyk, 1989, 1990). This was interpreted by Chocyk (1989, 1990) as the evidence indicating the origin of a significant matrix component from nearby rhyolitic volcanoes producing tephra. The tephra was possibly transported by aeolian-fluvial processes to the site of the basaltic trachyandesite eruption and deposited there. Such a weathered tephra component can be potentially detected based on its geochemistry. However, a closer inspection of the classification (Fig. 7) and the Harker-type diagrams (Fig. 8) of the Nieporaz–Brodła volcanics shows that the matrix geochemistry is related neither to the Zalas nor Miękinia or Dębnik rhyodacites. Although the content of incompatible elements such as Zr and Y are in the same range in the matrix and in the rhyodacites, the high concentration of compatible elements like Cr, Co and Ni suggests the importance of a component formed from basaltic trachyandesite weathering. Geochemical relation between the basaltic trachyandesites and siltstones is indicated by similar trace element ratios (Fig. 9) on the Zr/TiO_2 *vs.* Nb/Y discrimination plot (Winchester & Floyd, 1977). The use of the high field strength elements should significantly reduce the influence of late processes on the chemistry of volcaniclastics. The differences in the SiO_2, Al_2O_3 and Na_2O content are not reliable indicators because they might be attributed to weathering. The data of siltstone composition plot at the junction of the andesite and trachy- andesite fields, close to those of some of the lava flows. It is interesting that the interstitial glass also plots in the trachyandesite field despite its high-K rhyolitic composition (Fig. 9).

It can also be noted that the high-K rhyolitic siltstones plot in the same area as the interstitial high-K rhyolitic glass of basaltic trachyandesites (Fig. 7 and Table 2). The silica content is in the same range. However, the Harker-type diagrams (Fig. 8) clearly demonstrate that the volcaniclastic matrix does not contain differentiation products of fractional crystallisation of the basaltic trachyandesite magma.

The geochemical data are supplemented by petrography of the siltstones. The siltstones contain significant proportion of grains derived form weathering of crustal rocks, including white micas indicating admixture of terrigenic material (Fot. 7E). The pyromorphic quartz grains also indicate a small admixture of rhyolitic tephra, which was earlier suggested by Chocyk (1990). Considering the occurrence of horizontal lamination, good sorting, as well as the presence of quartz, alkali plagioclase and K-feldspar, accompanied by light and dark mica grains within clay matrix, the siltstones are interpreted as aeolian-fluvial sediments. The deposition consisted in gravitational filling of intra-clast spaces. The composition of terrigenic component corresponds to that of country rocks, represented by arkosic sandstones. The weathering and the occurrence of adhesive rims around breccia clasts (Fig. 5F) reflect palaeosoil formation (Chocyk, 1990). In turn, this reveals that the effusions of lava must have been separated by periods of quiescence between eruptions, probably recording a time span of some thousands of years. Such a time span between the formations of the major lava flows is recognised for example for the Holocene basaltic andesite volcanism in pull-apart basins of the Armenian highland (Karakhanian *et al.*, 2002). The basins there have been formed due to transformation of strike-slip dextral motion along the major intercontinental Pambak–Sevan–Sunik fault into local extension accompanied by subsidence (Philip *et al.*, 2001). The Sunik basin is filled with a thick felsic and basaltic andesite lava sequence of the Neogene to Pleistocene age. Volcanic vents in such a tectonic regime, can be also related to tail-cracks and horsetail-cracks (terminations of strike slip faults) or releasing bends along strike-slip faults (*e.g.*, Adıyaman *et al.*, 1998; Dhont *et al.*, 1998). The Holocene basaltic andesite lavas flowed from an array of monogenetic volcanoes located along the basin flank. Three lava generations are intercalated by soils and horizons containing Eneolithic culture objects used to date the flows (Karakhanian *et al.*, 2002).

In the Sławków and Nieporaz–Brodła basin, the eruption centres have not been identified. However, at the base of the volcanic sequence in Simota Valley, the sample (SIM-1) represents a thick rock body showing massive texture. Its position below platy lavas as well as coarser crystallinity suggests it to be a subvolcanic rock. The whole-rock geochemistry also resembles that of all other subvolcanic rocks (see paragraph: Tectonic setting). However, in the Simota basaltic trachyandesite, the orthopyroxene reaction coronas around clinopyroxene crystals are lacking, contrary to those observed in the Nadźwiedzia Góra sill. This feature indicates its crystallisation at shallower depths. The comparison of plagioclase microphenocryst sizes between the studied basaltic trachyandesites and basalt crystallised in a lava lake (Evans & Moor, 1968), roughly suggests their crystallisation at a depth of several metres (Fig. 6). Thus, the Simota sample could have crystallised in a lava lake. Rocks crystallised in lava lakes contain zones in which interstitial glass is well preserved (Evans & Moore, 1968), resembling the feature observed in the Simota basaltic trachyandesite. They usually form massive rock bodies preventing interstitial glass from water penetration and weathering, contrary to platy lavas, which can be easily penetrated by meteoric waters.

The Miękinia basaltic trachyandesite shares common geochemical features with other subvolcanic rocks in the studied area, namely the magnitudes of Sr, and Eu, as well as Ti and Nb anomalies; therefore, its lithostratigrafic value (Oberc & Parachoniak, 1962; Zajączkowski, 1972) is questionable and requires more study. Pioneering geological mapping was based on observations from the investigation pits (Zajączkowski, 1972), whereas now the rock outcrop is limited to the black variety studied here.

Geotectonic setting

Discrimination diagrams have been frequently used to identify the tectonic setting of ancient and recent igneous rocks (Pearce & Norry, 1979; Thomson & Flower, 1986; Benek *et al.*, 1996; Carmichael *et al.*, 1996; Gorton & Schandl, 2000). They are based on the observation that the concentrations and ratios of elements in magmas differ significantly depending on the tectonic setting of magma source. Of special interest are high field-strength elements (HFSE) like Ti, Nb, Ta, Zr, Y, Th and U, having high charge to radius ratio. The HFSE are usually unaffected by metasomatic alterations, a feature not to be ignored in a study of the volcanic series *ca.* 300 Ma old. In the volcanic arcs HFSE and HREE are left in subducted slab, whereas LILE and LREE are incorporated into subduction generated magmas by melting or by scavenging of elements by fluids from the mantle wedge (*e.g.*, Tatsumi *et al.*, 1995; Niu & O'Hara, 2009).

Zr *versus* Zr/Y diagram. The diagram Zr versus Zr/Y ratio has been proposed to differentiate basalts containing up to 52 wt. % SiO_2 between the mid-ocean ridge basalts (MORB), within-plate basalt (WPB) and island arc basalts (IAB) (Pearce & Norry, 1979). The difference in Zr/Y ratio between MORB and WPB was explained by magma source heterogeneities, whereas the Zr decrease in IAB relatively to MORB and WPB is the expression of a higher degree of partial melting beneath island arcs. It is the result of lowering of the mantle solidus, caused by the introduction of water into the island arc source region from subducted oceanic lithosphere (Pearce & Norry, 1979). Due to high Zr and Zr/Y ratio, the Nieporaz–Brodła basaltic trachyandesites plot within the WPB field (Fig. 10A). However, the results should be treated with caution, because the SiO_2 content of the studied rocks is between 51 and 55 wt. %, which is higher than the range originally used in this diagram. As evidenced by the same Zr/Y ratio (*ca.* 10) in the residual glass of the basaltic trachyandesite SIM-1 (Fig. 10A), fractional crystallisation does not change the Zr/Y ratio up to 76 wt. % of SiO_2, and indeed the Zr/Y ratio is capable of preserving the magma source characteristics up to the late stages of magma differentiation. The same would hold for variable

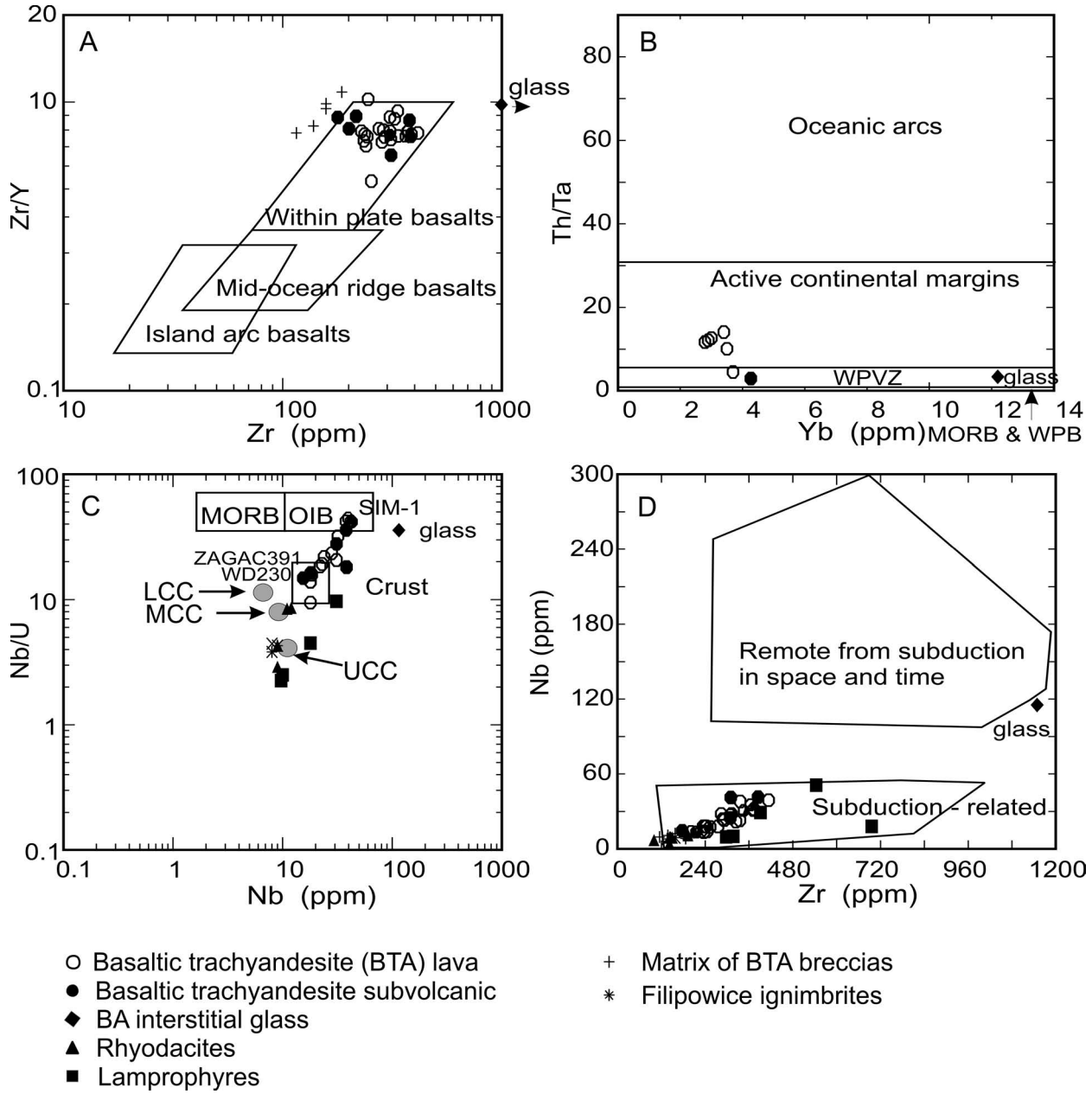

Fig. 10. The Nieporaz–Brodła volcanic series plotted on the tectonic setting discrimination diagrams: (**A**) Zr/Y versus Zr diagram for non-cumulate basalts (Pearce & Norry, 1979); (**B**) Th/Ta versus Yb diagram for felsic and intermediate volcanic rocks (Gorton & Schandl, 2000); WPVZ – within plate volcanic zone, MORB – mid-ocean ridge basalts; VPB – within-plate basalts; (**C**) Nb/U versus Nb diagram; LCC – lower, MCC – middle and UCC – upper continental crust (Rudnick & Gao, 2003), other reference data are from Carmichael *et al.* (1996); (**D**) Nb *versus* Zr for potassic and ultrapotassic rocks with $SiO_2 < 60\%$ (Thomson & Flower, 1986). Rock analyses by Czerny and Muszyński (1997, 1998) are also included, symbols like in Fig. 7

degree of partial melting. On the other hand, a progress of the fractional crystallisation increases significantly the Zr concentrations, for example in the sample SIM-1 it increases from 365 ppm in the bulk rock up to 1150 ppm in the residual glass. Concluding, different degree of fractional crystallisation or of partial melting results only in a horizontal shift of the projection points in the Zr *vs.* Zr/Y diagram, leaving unchanged the Zr/Y ratio for variable SiO_2 content. Therefore, the use of this diagram in the case of basaltic trachyandesites is fully justified.

Yb *versus* Th/Ta diagram. All HFSE except Th behave in very similar way in a given tectonic setting. Despite a low solubility of Th in subduction fluids, its concentration increases with respect to other HFSE (*e.g.*, Ta) in island arcs compared to within-plate rocks. This phenomenon is explained by Th derivation from sediments of the subducted slab, leading to a higher Th/Ta ratio in arc magmas, compared to those originating from within-plate setting (Gorton & Schandl, 2000). The diagram Yb versus Th/Ta ratio has been proposed to differentiate the WPB and MORB from within-plate volcanic zone (WPVZ) magmas, and those formed at active continental margins (ACM) and oceanic arc (OA). The Nieporaz–Brodła basaltic trachyandesites scatter within the WPVZ and ACM fields (Fig. 10B). As in-

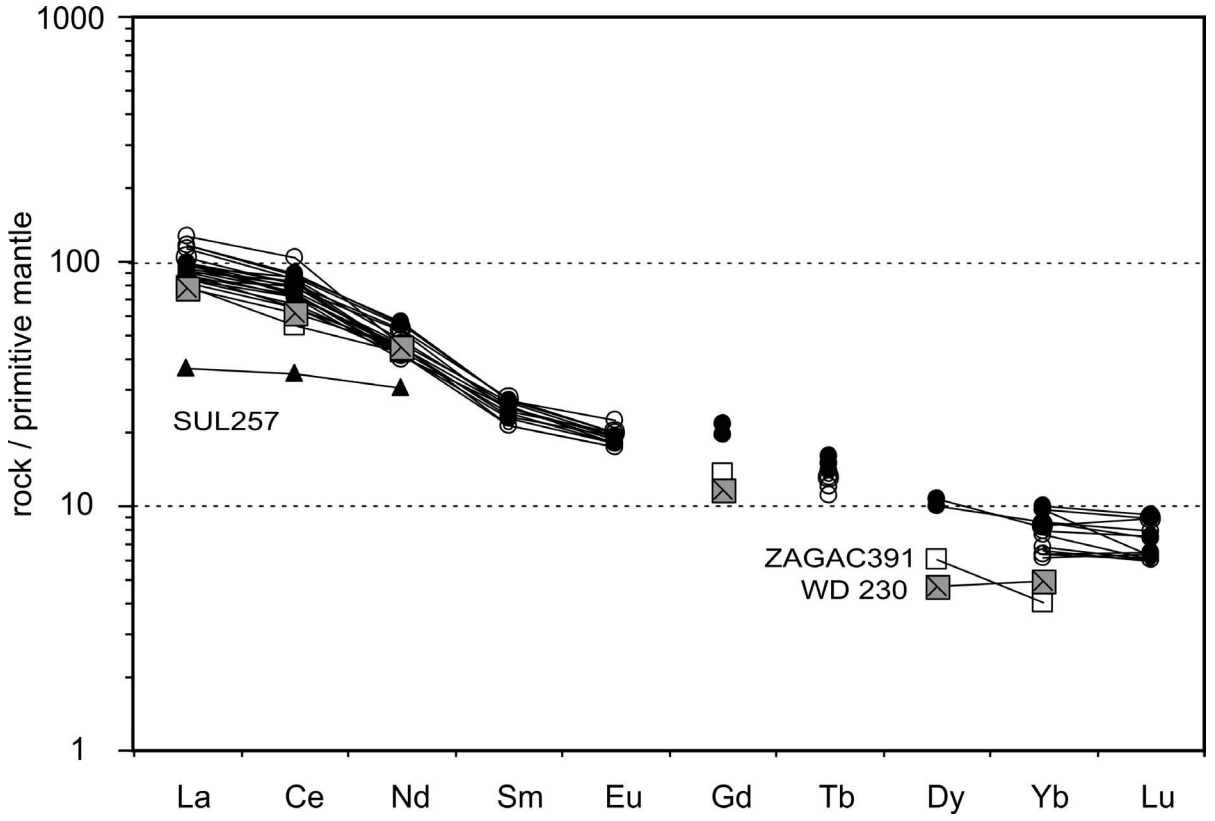

Fig. 11. Primitive mantle-normalized rare earth element (REE) diagram for the Nieporaz–Brodła basaltic trachyandesites plotted together with the Zalas rhyodacite. Values for primitive mantle are from McDonough and Sun (1995). All the rocks have strong LREE enrichment relative to HREE implying crustal or enriched mantle affinity. Rock analyses from Czerny and Muszyński (1997) are also included, symbols as in Fig. 7 with the exception of Sułoszowa (SUL257), Zagacie (ZAGAC391) and Wielkie Drogi (WD 230)

dicated by the position of the glass on the plot, the fractional crystallisation of basaltic trachyandesite mineral assemblage or partial melting is not influencing such a position (Fig. 10B). The basaltic trachyandesites position can be explained by the influence of crustal components on their source.

Nb *versus* Nb/U diagram. This conclusion is supported by the position of the basaltic trachyandesite plots on the Nb versus Nb/U diagram. The general geochemical data plotted there are from Carmichael *et al.* (1996). The samples form an array between oceanic island basalt (OIB) and crustal values. The average Nb/U value in these rocks is about 25, ranging from 15 to 45, except the Regulice outlier sample with Nb/U ~10 (U concentrations from Czerny & Muszyński, 1998). The relative depletion in Nb or enrichment in U in respect to MORB and most of OIBs magmas is clear from Fig. 10C. In turn, many basaltic trachyandesites have higher Nb/U ratios than the average continental crust (Fig. 10C). The average Nb/U ratios of the lower and upper continental crusts are 20 and 9, respectively (Taylor & McLennan, 1985), whereas Nb/U is 47±10 for both MORBs and OIBs (Hofmann *et al.*, 1986; Sims & DePaolo, 1997). The position of the Nieporaz–Brodła basaltic trachyandesite plots between OIB and crustal fields suggests the magma generation from enriched mantle source with varying amount of crustal component. The significant crustal component signature is observed in subvolcanics from Zagacie (ZAGAC391) and Wielkie Drogi (WD230), while less evolved are Simota (SIM-1) and Niedźwiedzia Góra rocks (Fig. 10C). In turn, the rhyodacites and lamprophyres fall in or close to the crustal field revealing their anatectic origin from rocks of the upper/middle continental crust composition (Fig. 10C). The continental crust compositions are according to Rudnick and Gao (2003). This is in agreement with the suggestion by Słaby *et al.* (2009) that the magmas were generated from two different sources: crust and enriched lithospheric mantle. For a mantle source, it is a requirement for any magma at equilibrium that the activity of silica in the magma has to match that defined by the olivine and orthopyroxene assemblage of the source region (Carmichael, 2002). Consistent with a mantle source would be the forsteritic composition ($Fo_{88–92}$) of the olivine phenocrysts (Carmichael, 2002). However, all the studied basaltic trachyandesites have fayalitic olivine on their liquidus, low MgO (<5 wt. %), and low compatible element Cr (63–148 ppm), and Ni (45–84 ppm) concentrations (Table 1), the features characteristic for evolved magmas.

Nb *versus* Zr diagram. Nb versus Zr is thought to distinguish between subduction-related and postcollisional settings and those associated with continental extension, remote from subduction in space and time (Pearce & Norry, 1979). The low Nb content suggests strong relation of the Nieporaz–Brodła rocks to subduction setting (Fig. 10D). Similar geochemical affinity of the Upper Carboniferous/

Permian volcanics from the Saar–Nahe Basin (Germany) led to a suggestion (Schmidberger & Hegner, 1999) that the Early Carboniferous (340–325 Ma) plate subduction continued up to Early Permian (*ca.* 300 Ma). However, such affinity of the magmatic rocks of Halle Volcanic Complex (dated at 307–294 Ma) was questioned as an evidence for active subduction due to geological data indicating crustal extension and rift setting (Romer *et al.*, 2001).

Summing up, in the Kraków area, the discrimination diagrams like those in Fig. 10A –D and others not shown here, are unable to label the tectonic position of the magmatic activity as understood in a simplistic way. The resulting settings range from within-plate (Fig. 10A), through transitional between within-plate and active continental margins (Fig. 10B), subduction-related zones (Fig. 10D) or generally suggesting involvement of a crustal component (Fig. 10C). Such a result is not surprising, because mobile belts are long-lived deformation zones, composed of an ensemble of varying crustal fragments, distributed over hundreds of kilometres inside continental convergent margins. The Late Carboniferous–Early Permian European magmatic province represents an example of such tectonic settings: the region is composed of a mosaic of microplates that moved and deformed in the overall plate convergence regime during the Variscan orogeny (Kalvoda *et al.*, 2008).

REE spider diagram. In this context, more promising seems to be analysing the variations of the entire spectrum of elements relaying on an internally coherent approach by comparing the studied rock trace element abundances to those of primitive mantle (Fig. 11). Such an approach (*e.g.*, Niu & O'Hara, 2009) is based on the fact that the excesses of Eu, Sr, Nb, Ta and Ti in the depleted MORB mantle (DMM) complement the well-known deficiencies of these elements in the bulk continental crust (BCC). Partial melting of amphibolite of MORB protolith during continental collision would lead to andesitic melts showing a remarkable similarity to the composition of BCC. Mineral composition of such amphibolite determines small but significant negative Eu and Sr anomalies (abundant plagioclase), accompanied by moderate Ti and high negative Nb and Ta anomalies (ilmenite) (Niu & O'Hara, 2009).

The needed numerical values, for example for the europium anomaly (Eu/Eu*) could be quantified by comparing the measured Eu (ppm) concentration with an expected Eu* concentration obtained by interpolating the normalized values from Sm and Nd, that is Eu/Eu*=2Eu/(Sm + Gd). Similarly, the strontium anomaly (Sr/Sr*) can be calculated as Sr/Sr*=2Sr/(Pr + Nd). The fact that the bulk partition coefficient during MORB mantle melting $D^{Nb} \approx D^{Th}$, $D^{Ta} \approx D^{U}$, $D^{Ti} \approx D^{Sm}$ allows to calculate numerical values of the Nb, Ta and Ti anomalies. For example, the Nb anomaly is a ratio of the measured and normalized concentration of Nb to Th (Nb/Th) (Niu & O'Hara, 2009). All the data were normalized to primitive mantle values (McDonough & Sun, 1995).

In the set of the data of the analysed samples and those from Czerny and Muszyński (1997), small Sr/Sr* ≈ 0.8 and significant Sr/Sr* ≈ 0.5 negative anomaly is noted in lavas and subvolcanic rocks, respectively. It is interesting that the Eu/Eu* anomaly is absent or very weak (Eu/Eu* ≈ 0.9–1.0). Moreover, the significant negative Nb (Nb/Th ≈ 0.3) and Ta (Ta/U ≈ 0.3) anomalies are observed in all the lavas and the subvolcanic Zagacie and Wielkie Drogi rocks. Other subvolcanic rocks show very small negative Nb (Nb/Th ≈ 0.9) and positive Ta (Ta/U ≈ 1.1) anomalies. These anomalies are accompanied by significant negative Ti (Ti/Sm ≈ 0.3) anomaly in all the rocks. The REE patterns of the studied rocks are steep, showing more than ten-fold LREE to HREE enrichment (Fig. 11). This pattern is characteristic for the enriched source. The high La to Yb ratio (La/Yb ≈ 10) is comparable to that observed in bulk continental crust, indicating a high degree of evolution of the studied rocks. The enrichment is higher in the lavas (La/Yb ≈ 11–20), compared to the subvolcanic equivalents (La/Yb ≈ 8–12).

Both Sr/Sr* and Eu/Eu* anomalies are controlled by plagioclase crystallisation but Eu/Eu* anomaly depends on oxidising conditions. During magma fractionation in oxidising conditions, Eu^{3+} behaves differently than Sr^{2+} what would result in Sr/Sr* negative and absence of Eu/Eu* anomaly.

Alternatively, the crystallisation of plagioclase in reducing conditions would lead to both Sr/Sr* and Eu/Eu* negative anomalies in the melt. Due to the fact that amphibole (but also garnet or orthopyroxene) controls the Eu/Eu* anomaly in the opposite sense to that of plagioclase (*e.g.*, Rollinson, 1993), the presence of, *e.g.* amphibole retaining in the source is required to compensate the Eu/Eu* anomaly.

In lavas, the LREE enrichment relative to HREE is higher than in the subvolcanic rocks from Niedźwiedzia Góra, Simota and Miękinia (steeper line in Fig. 11 for lavas). The difference was suggested to be a result of magma mixing (Czerny & Muszyński, 1997). However, higher Sr/Sr* and Eu/Eu* anomalies in the rocks from Simota, Miękinia and Niedźwiedzia Góra than in lavas, could be explained by plagioclase fractionation, whereas higher Nb, Ta and Ti anomalies in lavas could be attributed to Fe-Ti oxide fractionation. Both processes leading to these anomalies depend on water content in the magma. High water content evokes Fe-Ti oxide crystallization but is suppressing plagioclase precipitation, while degassing promotes plagioclase crystallization (Sisson & Grove, 1993). In the Simota, Miękinia and Niedźwiedzia Góra magmas, water was removed from the system, causing plagioclase crystallisation and fractionation. In lavas the water content was higher, suppressing early plagioclase crystallisation, thus enhancing effusion. Water pressure of 2 kbar is usually sufficient to delay plagioclase crystallisation and enhance Te, Fi-oxide crystallisation (Sisson & Grove, 1993; Carmichael, 2002). Crystallising hydrous liquid follows the classic calc-alkaline differentiation trend with little fractination of silicate minerals (Fig. 8).

The negative Nb, Ta, Ti anomalies and steep REE pattern due to high LREE and low HREE content in the studied samples (Fig. 11) suggest potential subduction-related setting or subduction-related metasomatism. However, the significant negative Sr anomaly contradicts direct involvement of subduction in active continental margin setting. The overall rock geochemistry resembles that of the recent post-collisional potassic volcanism in Tibet (Williams *et al.*, 2004). The magmatic activity in the Nieporaz–Brodła gra-

ben clearly postdates Variscan orogeny in the sense of the active oceanic slab subduction, but as strongly suggested by the volcanic rock geochemistry and high magma water content, must be related to slab detachment as the natural last stage in the gravitational settling of subducted lithosphere in a terminal stage of subduction. The orogen restructuring occurred by transformation of dextral strike-slip movement along the Hamburg–Kraków–Dobrogea Fault Zone into crustal extension. Nevertheless, an unequivocal classification of geodynamic context is difficult even for recent volcanism in most of the studied volcanic areas (*e.g.*, Lange & Carmichael, 1991); therefore, the conclusions on Stephanian/Early Permian volcanism shall be drawn only after definite palaeogeographical reconstruction of the southern Brunovistulian–Moesian–Istambul/Zonguldac terrane margin in the Permian is completed (Üstaömer & Robertson, 1993; Robertson *et al.*, 2004; Paszkowski *et al.*, 2007; Kalvoda *et al.*, 2008).

SUMMARY

The Kraków area in southern Poland is one of numerous centres of the Stephanian–Early Permian igneous activity in Europe. In Poland, the NW–SE trending transcontinental dextral strike-slip Hamburg–Kraków–Dobrogea fault system controlled the formation of sedimentary basins and volcanic activity. On the local scale in the Kraków area, the faulting resulted in the formation of NNE–SSW and NWW–SEE trending strike-slip fault systems', which fringe horsts and grabens. The Sławków and Nieporaz–Brodła grabens formation in the west was accompanied by the uplift of the Dębnik anticline in the east. A deep erosion of the uplifted area brought up to the surface a diabase sill (Niedźwiedzia Góra) and two rhyodacite intrusions (Dębnik and Zalas). Large size of the Dębnik intrusion is evidenced by extensive contact metamorphism aureole, some hundreds of meters thick.

Erosional remnants of the volcano-sedimentary succession occur in the Sławków and Nieporaz–Brodła graben system, where the variations of sedimentary facies reveal that tectonic activity was contemporaneous with the volcanism. The position of the Miękinia rhyodacite within the subsided area and overlying the fanglomerates suggests that the rhyodacite represents a lava dome.

In the Nieporaz–Brodła graben, three basaltic trachyandesite a-a lava flows with volcaniclastics reach *ca.* 150 m in thickness. The lava flows become scoriaceous upwards with angular scoriaceous rubbles forming autoclastic breccias at the top. The breccias are framework-supported, composed of large lava blocks set in siltstone matrix. The siltstones are interpreted as aeolian-fluvial inner tuffaceous sediments by considering the occurrence of horizontal lamination, good sorting, as well as the presence of quartz (including pyromorphic) and K-feldspar accompanied by light and dark mica grains in clay matrix. The weathering and the occurrence of adhesive rims around breccia clasts reflect palaeosoil formation. Thus, the lava flows must have been separated by periods of quiescence, probably recording a time span of some thousands of years. The eruptions were effusive, although scoriaceous lavas and rubbles indicate a relatively high volatile content of the lavas. The primary water content before eruption had to be over 2 wt. %, because only when assuming such a water content of basaltic trachyandesite magmas the thermodynamic crystallisation modelling predicts well the type and order of the crystallising phases, and adequately reflects the natural phenocryst composition. All erupted basaltic trachyandesites had fayalitic olivine (plus Fe-Ti oxides) on the liquidus, the first crystallising phase due to water suppression of plagioclase crystallisation up to the upper crustal levels. These were followed by labradorite plagioclases stabilised by high water pressure. After adiabatic magma ascent from its source, such water-rich magma upon approaching the surface over-saturated and exsolved aqueous fluid. During such a decompression stage, spinel, more sodic plagioclase, augite, ilmenite, apatite and K-feldspar crystallised as well as the remaining melt reached high-K rhyolitic composition. Thus, the high potassium content of these volcanics is a primary feature reflecting the source composition and the way of magma evolution and its consequence was late irregular potassium metasomatism. This process caused the replacement of olivine by K-rich iddingsite and alteration of glass. However, some rocks still contain microscopically isotropic homogenous interstitial glass. This glass has high-K rhyolitic composition and is strongly enriched in incompatible trace elements (*e.g.*, Zr,Y) showing that it represents a highly fractionated residual melt fraction of basaltic trachyandesite magma. Thus, the glass geochemistry can be used to trace the trend of fractional crystallisation, indicating that co-occurring high-K felsic rocks are not derived from the same magma.

The studied rocks form an uniform group including the samples from Wielkie Drogi and Zagacie. They have calc-alkaline to alkaline affinity and are medium-K to high-K basaltic andesites (or basaltic trachyandesites), the majority of which can be classified as shoshonites due to appropriately high K/Na ratios. All these rocks have steep REE pattern with more than ten-fold enrichment of LREE relatively to HREE (La/Yb = 8–18). The REE pattern and negative Nb, Ta and Ti anomalies suggest subduction-related characteristics, but the significant negative Sr/Sr* » 0.5–0.80 and the described geotectonic context are not consistent with such an environment. The small Eu/Eu* » 0.9–1.0 and negative Sr/Sr* anomalies suggest melting of amphibole in the source and late fractionation of plagioclase. Ilmenite retained in the source or fractionated could be responsible for negative Nb, Ti and Ta anomalies.

A close spatial and temporal association of the volcanism and the basin formation suggest that strike-slip dextral motion along the major Hamburg–Kraków–Dobrogea fault was transformed into local extension accompanied by subsidence, the features which characterise a pull-apart basin formation.

CONCLUSIONS

1. In the Sławków and Nieporaz–Brodła basins, basaltic trachyandesite (BTA) lava flows represent a-a lavas with thick autoclastic breccias. The matrix of the breccias is com-

posed of aeolian-fluvial siltstones consisting of weathering products of BTA with an admixture of reworked Stephanian arkose and a minor felsic tephra component. The weathering of breccias and the development of palaeosoil horizons indicate that the lava flows must have been separated by quiescence periods lasting at least some thousands of years.

2. Three final stages of magma evolution are recorded in the basaltic trachyandesite petrography. Their modelling reveals that in the first stage fayalitic olivine phenocrysts followed by spinel appeared at the liquidus at shallow crustal depths. The nucleation of labradorite core of plagioclases started before water exsolution. In the second rapid decompression stage during ascent in volcanic conduit, the BTA magma lost water and consequently more sodic plagioclase together with spinel, augite, apatite and ilmenite precipitated. In this stage the eruptibility limit was reached. The last stage, marking solidification at the surface, yields apatite, K-feldspar (often rimming plagioclase) and residual glass. Such an evolution can be modelled only by assuming substantial water content (over 2 wt. %) in the BTA magma originated from a source containing hydrous mineral phases (*i.e.*, amphibole or phlogopite).

3. The shift of the trace element content from bulk BTA magma to the interstitial glass composition reveals the trend of the BTA fractional crystallisation (FC) and evidences that co-occurring potassium rhyodacites can not be the products of FC of the BTA magma, though clear spatial and temporal relationship between both series indicates common processes leading to magma generation.

4. The high potassium content of these BTA volcanics is a primary feature reflecting the magma source geochemistry and the magma evolution toward high-K composition, and its consequence was the later patchy potassium metasomatism related to water exsolution during the ascent of magma to the surface.

5. The BTA are the products of crystallisation of highly evolved magma, as evidenced by the fayalitic composition of the olivine phenocrysts and bulk rock low MgO (<5 wt. %), Cr and Ni content. The intermediate calc-alkaline to alkaline affinity of BTA, high-K content, significant LREE *vs.* HREE enrichment, and Nb and Ti negative anomalies suggest metasomatism in a subduction-related setting. However, strong Sr negative anomaly and geological data are not consistent with active subduction. The BTA geochemistry simply indicates remarkable role of water in magma formation and evolution.

6. LREE enrichment, HREE depletion, stronger Nb, Ta and Ti anomalies, and weaker Sr/Sr* and Eu/Eu* anomalies in the lavas than in the subvolcanic equivalents indicate that the lava evolved from magmas with higher water content. The water caused Fe-Ti oxide fractionation and suppressed plagioclase crystallisation. Subvolcanic rocks evolved after water exsolution from the magma, which resulted in minor plagioclase fractional crystallisation at shallow depths.

7. A close spatial and temporal association of the volcanism with the basin formation suggests that the strike-slip dextral motion along the major Hamburg–Kraków–Dobrogea fault was transformed into local extension accompanied by subsidence, which is typical for a pull-apart basin formation.

Acknowledgements

The authors thank Prof. W. Moryc for providing the sample from the Zagacie borehole. The historical Sułoszowa and Wielkie Drogi logs are inherited from the passed Prof. Czesław Harańczyk and Prof. Antoni Gaweł collections. We would like to thank Prof. Friedrich Finger and Dr. Dan Topa for WDS and XRF analyses, and Prof. Bernhard Schultz for LA ICP MS analyses. The Jagiellonian University and the VENTS Field Workshops, supported by the Polish Ministry of Science and Higher Education and the German Research Foundation (DFG), financed this work. The work highly benefited from the Synthesis programme and discussion with Åke Johansson from the Laboratory for Isotope Geology, Swedish Museum of Natural History. The manuscript benefited from constructive reviews by Prof. Ewa Słaby and Dr. Marek Awdankiewicz, as well as from the comments of Prof. Wojciech Narębski and Dr. Bartosz Budzyń.

REFERENCES

Adıyaman, Ö., Chorowicz, J. & Köse, O., 1998. Relationships between volcanic patterns and neotectonics in Eastern Anatolia from analysis of satellite images and DEM. *Journal of Volcanology and Geothermal Research*, 85: 17–32.

Awdankiewicz, M., 1999a. Volcanism in a late Variscan intramontane trough: Carboniferous and Permian volcanic centres of the Intra-Sudetic Basin, SW Poland. *Geologia Sudetica*, 32: 13–47.

Awdankiewicz, M., 1999b. Volcanism in a late Variscan inter-m ountain trough: the petrology and geochemistry of the Carboniferous and Permian volcanic rocks of the Intra-Sudetic Basin, SW Poland. *Geologia Sudetica*, 32: 83–111.

Awdankiewicz, M., Awdankiewicz, H., Kryza, R., Rodionov, N. & Timmerman, M., 2009. Ar-Ar and SHRIMP constraints on the age of Late Palaeozoic intermediate and silicic dykes and sills in the Sudetes. In: Lewandowska, A. & Rospondek, M. J. (eds), *Permo–Carboniferous volcanism of the Kraków region. VENTS4 Field Workshop, Kraków, 21st–24th May 2009*. *Mineralogia, Special Papers*, 34: 9.

Awdankiewicz, M. & Kryza, R., 2010a. The Chełmiec subvolcanic intrusion (Intra-Sudetic Basin, SW Poland): preliminary SHRIMP zircon age. In: Awdankiewicz, M. & Awdankiewicz, H. (eds), *Lamprophyres and related mafic hybabyssal rocks: current petrological issues, 14th-17th October 2010. Mineralogia, Special Papers*, 37: 69.

Awdankiewicz, M. & Kryza, R., 2010b. The Góry Suche Rhyolitic Tuffs (Intra-Sudetic Basin, SW Poland): preliminary SHRIMP zircon age. In: Awdankiewicz, M. & Awdankiewicz, H. (eds), *Lamprophyres and related mafic hybabyssal rocks current: petrological issues, 14th-17th October 2010. Mineralogia, Special Papers*, 37: 70.

Benek, R., Kramer, W., McCann, T., Scheck, M., Negandank, J. W., Korich, D., Huebscher, H. D. & Bayer, U., 1996. Permo-Carboniferous magmatism of the Northeast German Basin. *Tectonophysics*, 266: 379–44.

Birkenmajer, K., 1952. Kontakt melafiru z arkozą kwaczalską we wzgórzu Belweder koło Poręby Żegoty. (In Polish). *Biuletyn Instytutu Geologicznego*, 80: 5–14.

Birkenmajer, K., 1964. Palaeomagnetic studies of Polish rocks. (In Polish, English summary). *Rocznik Polskiego Towarzystwa Geologicznego*, 34: 225–244.

Bogacz, K., 1980. Tectonics of the Palaeozoic rocks of the Dębnik region. (In Polish, English summary). *Rocznik Polskiego Towarzystwa Geologicznego*, 50: 183–208.

Bukowy, S. & Cebulak, S., 1964. New data concerning magmatism of Silesian–Cracovian Anticlinorium. (In Polish, English summary). *Kwartalnik Geologiczny*, 7: 41–94.

Bukowy, S., 1975. *Dokumentacja geologiczna otworu Sułoszowa* (In Polish, archival manuscript). Państwowy Instytut Geologiczny, Sosnowiec.

Carmichael, I. S. E., 2002. The andesite aqueduct: perspectives on the evolution of intermediate magmatism in west-central (105–99°W) Mexico. *Contributions to Mineralogy and Petrology*, 143: 641–663.

Carmichael, I. S. E., Lange, R. A., & Luhr, J. F., 1996. Quaternary minettes and associated volcanic rocks of Mascota, western Mexico: a consequence of plate extension above a subduction modified mantle wedge. *Contributions to Mineralogy and Petrology*, 124: 302–333.

Chocyk, M., 1989. *Charakterystyka mineralogiczna i petrograficzna tufów z Regulic.* (In Polish). Unpublished MSc. Thesis, Uniwersytet Jagielloński, Kraków, Poland, 130 ms. pp.

Chocyk, M., 1990. Późnopaleozoiczne utwory piroklastyczne z Regulic k. Alwerni. (In Polish). *Przegląd Geologiczny*, 38: 390–393.

Cichoń, G., 1982. Minerały wtórne w melafirach z Rudna koło Krzeszowic. (In Polish). *Prace Mineralogiczne Komisji Nauk Mineralogicznych PAN*, 73: 7–53.

Czerny, J. & Muszyński, M., 1997. Co-magmatism of the Permian volcanities of the Krzeszowice Area in the light of petrochemical data. *Mineralogia Polonica*, 28: 3–25.

Czerny, J. & Muszyński, M., 1998. New petrochemical data on lamprophyres from the margin of the Upper Silesia Coal Basin. *Mineralogia Polonica*, 29: 67–75.

Dżułyński, S., 1955. O formie porfirów zalaskich. (In Polish). *Biuletyn Instytutu Geologicznego*, 97: 9–38.

Dhont, D., Chorowicz, J., Yürür, T., Froger, J.-L., Köse, O. & Gündogdu, N., 1998. Emplacement of volcanic vents and geodynamics of Central Anatolia, Turkey. *Journal of Volcanology and Geothermal Research*, 85: 33–54.

Evans, B. W. & Moore, J. G., 1968. Mineralogy as a function of depth in the prehistoric Macaopuhi tholeiitic lava like, Hawaii. *Contributions to Mineralogy and Petrology*, 17: 85–115.

Falenty, A., 2004. *Modelowanie geochemiczne pochodzenia stopu zasadowego wulkanizmu okolic Krakowa.* (In Polish). Unpublished MSc. Thesis, Warsaw University, 53 ms. pp.

Frost, R. B., Andersen, D. J. & Lindsley, D. H., 1988. Fe-Ti oxide silicate equilibria: Assemblages with fayalitic olivine. *The American Mineralogist*, 73: 727–740.

Furgal, S. A. & McMillan, N. J., 2001. Magmatic iddingsite changes in H_2O in magma chamber prior to eruption. *Annual Meeting of the Geological Society of America, 5–8th November 2001, Boston, Massachusetts. Paper* No. 155-0.

Gaweł, A., 1953. Jaspisy z diabazu z Niedźwiedziej Góry. (In Polish). *Acta Geologica Polonica*, 3: 1–32.

Ghiorso, M. S. & Sack, R. O., 1995. Chemical mass transfer in magmatic processes. IV. A revised and internally consistent thermodynamic model for the interpolation and extrapolation of liquid-solid equilibria in magmatic systems at elevated temperatures and pressures. *Contributions to Mineralogy and Petrology*, 119: 197–212.

Gniazdowska, K., 2004. *Modelowanie pochodzenia stopu kwaśnego wulkanizmu okolic Krakowa*. (In Polish). Unpublished MSc. Thesis, Warsaw University.

Gradziński, R., 1993. *Geological map of Cracov region*. Geological Museum, Polish Academy of Sciences, Kraków.

Gorton, M. P. & Schandl, E. S., 2000. From continents to island arcs: A geochemical index of tectonic setting for arc-related and within-plate felsic to intermediate volcanic rocks. *The Canadian Mineralogist*, 38: 1065–1073.

Harańczyk, C., 1989. Rozwój wulkanizmu krakowskiego. (In Polish). In: Rutkowski, J. (ed.), *Przewodnik LX Zjazdu Polskiego Towarzystwa Geologicznego, Kraków,14-16 września 1989.* Wydawnictwo Akademii Górniczo-Hutniczej, Kraków: 51–57.

Harańczyk, C., Lankosz, M., & Wolska, A., 1995. Granodioryt jerzmanowicki, porfiry i kruszce. (In Polish). *Rudy i Metale Nieżelazne*, 40: 334–341.

Heflik, W., 1960. Charakterystyka petrograficzna diabazów i melafirów z Miękini. (In Polish). *Biuletyn Instytutu Geologicznego*, 155: 203–222.

Hofmann, A. W., Jochum, K. P., Seufert, M. & White, W. M., 1986. Nb and Pb in oceanic basalts: new constraints on mantle evolution. *Earth and Planetary Science Letters*, 79: 33–45.

Housh, T. B. & Luhr, J. F., 1991. Plagioclase-melt equilibria in hydrous systems. *The American Mineralogist*, 76: 477–492.

Jarmołowicz-Szulc, K., 1984. Datowania metodą K-Ar skał NE obrzeżenia Górnośląskiego Zagłębia Węglowego. (In Polish). *Kwartalnik Geologiczny*, 28: 749–750.

Jarmołowicz-Szulc, K., 1985. Badania geochronologiczne K-Ar skał magmowych północno-wschodniego obrzeżenia Górnośląskiego Zagłębia Węglowego. (In Polish). *Kwartalnik Geologiczny*, 29: 343–354.

Kalvoda, J., Bábek, O., Fatka, O., Leichmann, J., Melichar, R., Nehyba, S. & Spacek, P., 2008. Brunovistulian terrane (Bohemian Massif, Central Europe) from late Proterozoic to late Paleozoic: a review. *International Journal of Earth Sciences*, 97: 497–518.

Karakhanian, A., Djrbashian, R., Trifonov, V., Philip, H., Arakelian, S. & Avagian, A., 2002. Holocene-historical volcanism and active faults as natural risk factors for Armenia and adjacent countries. *Journal of Volcanology and Geothermal Research*, 113: 319–344.

Kiersnowski, H., 2001. Permian-Triassic deposits of the Liplas–Tarnawa basins. (In Polish, English summary). In: Matyja, H. (ed.), *Paleozoic Basement of Central Segment of the Polish Outer Carpathians (Liplas–Tarnawa region). Prace Państwowego Instytutu Geologicznego*, 174: 87–100.

Kotas, A., 1982. Zarys budowy geologicznej Górnośląskiego Zagłębia Węglowego. (In Polish). In: Rożkowski, A. & Ślósarz, J. (eds), *Przewodnik LIV Zjazdu Polskiego Towarzystwa Geologicznego, Sosnowiec 1982.* Wydawnictwa Geologiczne, Warszawa: 45–72.

Kozłowski, S., 1953. Nowe znaleziska porfiru. (In Polish). *Przegląd Geologiczny*, 2: 22–23.

Lange, R. A. & Carmichael, I. S. E., 1991. A potassic volcanic front in western Mexico: the lamprophyric and related lavas of San Sebastian. *Geological Society of America Bulletin*, 103: 928-940.

Le Maitre, R., Streckeisen, A., Zanettin, B., Le Bas, M. J., Bonin, B., Bateman, P., Belleini G., Dudek, A., Efremova, S., Keller, J., Lameyre, J., Sabine, P. A., Schmid, R., Sorensen, H. & Wooley, A. R., 2002. *A classification of igneous rocks and glossary of terms: Recommendations of the International Union of Geological Science Subcommission on the Systematics of Igneous Rocks.* Blackwell, Oxford, 236 pp.

Lewandowska, A., 1991. Minerals of the zone of altered Devonian dolomites from Dubie near Kraków (Southern Poland). *Mineralogia Polonica*, 22: 29–40.

Lewandowska, A., 2009. Stop 1. Dubie - operating quarry. In: Lewandowska, A. & Rospondek, M. J. (eds), *Permo–Carboniferous volcanism of the Kraków region. VENTS4 Field Workshop, Kraków, 21st–24th May 2009*. *Mineralogia, Special*

Papers, 34: 50–52.

Lewandowska, A., Banaś, M. & Zygoń, K., 2007. K-Ar dating of amphiboles from andesites of complex dyke in Dubie (Southern Poland). *Geochronometria*, 27: 11–15.

Lewandowska, A. & Rospondek, M. J., 2007. Late Carboniferous–early Permian magmatic rocks of the Kraków area, southern Poland. In: Rapprich, V. & Řídkošil, T. (eds), *Volcanic systems within the European Permocarboniferous intermountain basins and their basement, VENTS 2007, Turnov–Sedmihorky, Abstracts and excursion guide.* Muzeum Českého ráje v Turnově, 2007, Turnov–Sedmihorky: 15.

Lewandowska, A. & Rospondek, M. J., 2009. Stop 3. Regulice–Czarna Góra abandoned quarry. In: Lewandowska, A. & Rospondek, M. J. (eds), *Permo–Carboniferous volcanism of the Kraków region. VENTS4 Field Workshop, Kraków, 21st–24th May 2009*. *Mineralogia, Special Papers*, 34: 53–55.

Lewandowska, A., Rospondek, M. J., Finger, F., Schulz, B., & Nawrocki, J., 2008. Petrogenesis of Late Carboniferous/Early Permian basaltic trachyandesites from the Kraków area, Southern Poland. In: Breitkreuz, C., Haffmann, U., Renno, A. D. & Stanek, K. (eds), *Volcanic systems within the European Permocarboniferous intermountain basins and their basement, 3rd VENTS Field Workshop, Freiberg, Germany, 15–18th May 2008.* Institute for Geology, TU Bergakademie Freiberg: 10–11.

Lipiarski, I., 1970. The Carboniferous–Permian Boundary in the Eastern Part of the Cracow–Silesian Coal Basin. *Bulletin de L'Académie Polonaise des Sciences*, 28: 173–178.

Luhr, J. F., 1990. Experimental phase relations of water- and sulfur-saturated arc magmas and the 1982 eruptions of El Chichon volcano. *Journal of Petrology*, 31: 1071–1114.

Łapot, W., 1992. Zróżnicowanie petrograficzne tonsteinów Górnośląskiego Zagłębia Węglowego. (In Polish). *Prace Naukowe Uniwer- sytetu Śląskiego*, 1326: 1-110.

McDonough, W. F. & Sun, S., 1995. The composition of the Earth. *Chemical Geology*, 120: 223–253.

Markiewicz, J., 2001. Magmatic rocks. In: Podemski, M. (ed.), *Palaeozoic Porphyry Molybdenium-Tungsten Deposit in the Myszków Area, Southern Poland. Polish Geological Institute, Special Papers*, 6: 31–43.

Moore, G. & Carmichael, I. S. E., 1998. The hydrous phase equilibria (to 3 kbar) of an andesite and basaltic andesite from western Mexico: constraints on water content and conditions of phenocryst growth. *Contributions to Mineralogy and Petrology*, 130: 304–319.

Muszyński, M., 1995. Systematic position of igneous rocks from the northern margin of the Upper Silesian Coal Basin. *Mineralogia Polonica*, 26: 33–49.

Muszyński, M. & Czerny, J., 1997. Semilamprofir minettopodobny z doliny Szklarki koło Krakowa. (In Polish). *Przegląd Geologiczny*, 45: 1024–1027.

Muszyński, M. & Pieczka, A., 1992. Hornblende andesites and dacites from Dubie near Krzeszowice. *Mineralogia Polonica*, 23: 43–63.

Muszyński, M. & Pieczka, A., 1996. Potassium-bearing volcanic rocks from the northern margin of the Krzeszowice Trough. *Mineralogia Polonica*, 27: 3–24.

Nawrocki, J., Fanning, M., Lewandowska, A., Polechońska, O. & Werner, T., 2008. Palaeomagnetism and the age of the Cracow volcanic rocks (S Poland). *Geophysical Journal International*, 174: 475–488.

Nawrocki, J. Krzemiński, L., Pańczyk, M., 2010. ^{40}Ar-^{39}Ar ages of selected rocks and minerals from the Kraków-Lubliniec Fault Zone, and its relation to Palaeozoic structural evolution of the Małopolska and Brunovistulian terranes (S Poland). *Geological Quaterly*, 54: 289-302.

Nawrocki J., Lewandowska A., & Fanning M., 2007. Isotope and paleomagnetic ages of the Zalas rhyodacites (S Poland). (In Polish, English summary). *Przegląd Geologiczny*, 55: 475–478.

Nawrocki, J., Polechońska, O., Lewandowska, A. & Werner, T., 2005. On the palaeomagnetic age of the Zalas laccolith (southern Poland). *Acta Geologica Polonica*, 55: 229–236.

Nicholls, J. & Carmichael, I. S. E., 1969. A commentary on absarokite–shoshonite–banakites series of Wyoming. *Schweizerische Mineralogische und Petrologische Mitteilungen*, 49: 47–64.

Niu, Y. & O'Hara, M. J., 2009. MORB mantle hosts the missing Eu (Sr, Nb, Ta and Ti) in the continental crust: New perspectives on crustal growth, crust–mantle differentiation and ch e-mical structure of oceanic upper mantle. *Lithos*, 112: 1–17.

Oberc, A. & Parachoniak, W., 1962. The melaphyre from Filipowic. (In Polish, English summary). *Rocznik Polskiego Towarzystwa Geologicznego*, 32: 57–72.

Parachoniak, W. & Wieser, T., 1985. The nature and origin of Filipowice Tuffs. In: Wieser, T. (ed.), *Carpatho-Balkan Geological Association XIII Congress*, *Geological Institute, Kraków*. Wydawnictwa Geologiczne. Warszawa: 16–22.

Parachoniak, W. & Wieser, T., 1992. Adular z wakuoli melafirów z Alwerni. (In Polish). *Sprawozdania z Posiedzeń Komisji Naukowych PAN, Oddział w Krakowie*, 34: 236–239.

Paszkowski, M., Matyasik, I. & Rospondek, M. J., 2008. Comparison of gases and source rocks from two tectonically dismembered segments of Pennsylvanian coal basin. *61 Türkiye Jeoloji Kurultayi Bildirileri, Ankara, Turkey, 24–28 Mart 2008*: 71.

Pearce, J. A. & Norry, M. J., 1979. Petrogenetic implications of Ti, Zr, Y, and Nb variations in volcanic rocks. *Contributions to Mineralogy and Petrology*, 69: 33–47.

Philip, H., Avagyan, A., Karakhanian, A., Ritz, J.-F. & Rebai, S., 2001. Estimating slip rates and recurrence intervals for strong earthquakes along an intracontinental fault: example of the Pambak-Sevan-Sunik fault (Armenia). *Tectonophysics*, 343: 205– 232.

Podemski, M., 2001. Palaeozoic Porphyry Molybdenium-Tungsten Deposit in the Myszków Area, Southern Poland. *Polish Geological Institute, Special Papers*, 6, 1–88 p.

Robertson, A. H. F., Üstaömer, T., Pickett, E. A., Collins, A. S., Andrew, T. & Dixon, J. E., 2004. Testing models of Late Palaeozoic–Early Mesozoic orogeny in Western Turkey: support for an evolving open-Tethys model. *Journal of the Geological Society*, 161: 501–511.

Rollinson, H., 1993. *Using Geochemical Data: Evaluation, Presentation, Interpretation.* Longman & Wiley, NewYork, 352 pp.

Romer, R. L., Föster, H. J., & Breitkreutz, C., 2001. Intracontinental extensional magmatism with a subduction fingerprint: the late Carboniferous Halle Volcanic Complex (Germany). *Contributions to Mineralogy and Petrology*, 141: 201–221.

Rospondek, M. J., Lewandowska, A., Chocyk-Jamińska, M. & Finger, F., 2004. Residual glass of high-K basaltic andesites (shoshonites) from the Nieporaz–Brodla graben near Krzeszowice. *Prace Specjalne Polskiego Towarzystwa Mineralogicznego*, 24: 337–340.

Rospondek, M. J., Lewandowska, A., & Marynowski, L., 2009. Fate of organic matter during contact metamorphism induced by Permian magmatic activity in the Dębnik anticline, Southern Poland. In: Lewandowska, A. & Rospondek, M. J. (eds), *Permo–Carboniferous volcanism of the Kraków region. VENTS4 Field Workshop, Kraków, 21st–24th May 2009*.

Mineralogia, Special Papers, 34: 22–23.

Roszek, H. & Siedlecka, A., 1966. Permian volcanites at Zbójnik near Nieporaz (Silesia–Cracow region). (In Polish, English summary). *Rocznik Polskiego Towarzystwa Geologicznego*, 36: 35–69.

Rozen, Z., 1909. Dawne lawy Wielkiego Księstwa Krakowskiego. (In Polish). *Rozprawy Wydziału Matematyczno-Przyrodniczego PAU,* 9A: 293–368.

Rudnick, R. L. & Gao, S., 2003. Composition of the continental crust. In: Holland, H. D. & Turekian, K. K. (eds), *Treatise on Geochemistry*, 3: 31–64.

Rutherford, M. J. & Devine, J. D., 1988. The May 18, 1980 eruption of Mount St. Helens. 3. Stability of amphibole in the magma chamber. *Journal of Geophysical Research*, 93: 11949–11959.

Rutherford, M. J., Sigurdsson, H., Carey, S. & Davis, A., 1985. The May 18, 1980 eruption of Mount St. Helens melt composition and experimental phase equlibria. *Journal of Geophysical Research*, 90: 2929–2947.

Rutkowski, J., 1958. Uwagi o melafirach Poręby i Mirowa koło Alwerni. (In Polish). *Kwartalnik Geologiczny*, 2: 267–278.

Schmidberger, S. & Hegner, S. E., 1999. Geochemistry and isotope systematics of calc-alkaline volcanic rocks from the Saar–Nahe basin (SW Germany) – implications for Late-Variscan orogenic development. *Contributions to Mineralogy and Petrology*, 135: 373–385.

Siedlecka, A., 1964. Permian in the north-eastern border of the Upper Silesia Coal Besin. (In Polish, English summary). *Rocznik Polskiego Towarzystwa Geologicznego*, 34: 309–394.

Siedlecki, S., 1954. Palaeozoic formations of the Cracow region. (In Polish, English summary). *Biuletyn Instytutu Geologicznego*, 73: 1–415.

Siedlecki, S. & Żabiński, W., 1953. Tuf melafirowy i niższy pstry piaskowiec w Alwerni. (In Polish). *Acta Geologica Polonica*, 3: 441–468.

Sims, K. W. W. & DePaolo, D. J., 1997. Inferences about mantle magma sources from incompatible element concentration ratios in oceanic basalts. *Geochimica et Cosmochimica Acta*, 61: 765–784.

Sission, T. W. & Grove, T. L., 1993. Temperatures and H_2O contents of low-MgO high alumina basalts. *Contributions to Mineralogy and Petrology*, 113: 167–184.

Skowroński, A., 1974. Oznaczenie wieku bezwzględnego tzw. porfirów z Zalasu metodą śladów rozszczepienia jąder uranu. (In Polish). *Sprawozdania z Posiedzeń Komisji Naukowych PAN, Oddział w Krakowie*, 17: 236–237.

Słaby, E., 1990. Adularia from Miękinia. (In Polish, English summary). *Archiwum Mineralogiczne*, 46: 55–66.

Słaby, E., 2000. Adularia and albite – hydrothermal feldspars from Zalas and Mięknia rocks. *Prace Specjalne Polskiego Towarzystwa Mineralogicznego*, 17: 94–96.

Słaby, E., Breitkreuz, C., Żaba, J., Domańska-Siuda, J., Gaidzik, K., Falenty, K. & Falenty, A., 2010. Magma generation in an alternating transtensional–transpressional regime, the Kraków–Lubliniec Fault Zone, Poland. *Lithos*, 119: 51-268.

Słaby, E., Falenty, K., Falenty, A., Breitkreuz, C., Bachliński, R. & Domańska-Siuda, J., 2007. Model of magma generation and differentiation in Permian volcanic rocks of the Kraków area. *Mineralogical Society of Poland, Special Papers*, 31: 247–249.

Słaby, E., Żaba, J., Falenty, K., Falenty A., Breitkreuz, C. & Domanska-Siuda, J., 2009. The origin and the evolution of magmas of Permo–Carboniferous volcanism of the Kraków region. In: Lewandowska, A. & Rospondek, M. J. (eds), *Permo-Carboniferous volcanism of the Kraków region. VENTS4 Field Workshop, Kraków, 21st–24th May 2009*. *Mineralogia, Special Papers*, 34: 47–48.

Tatsumi, Y., Kosligo, T., & Nohda, S., 1995. Formation of the third volcanic chain in Kamchatka. Generation of unusual subduction-related magmas. *Contributions to Mineralogy and Petrology*, 120: 117–128.

Taylor, S. R. & McLennan, S. M., 1985. *The continental crust: its composition and evolution*. Blackwell, Oxford, 312 pp.

Thomson, R. N. & Fowler, M. B., 1986. Subduction related shoshonitic and ultrapotassic magmatism: a study of Siluro–Ordovician syenites from the Scottish Caledonides. *Contributions to Mineralogy and Petrology*, 94: 507–522.

Üstaömer, T. & Robertson, A. H. F., 1993. A Late Paleozoic–Early Mesozoic marginal basin along the active southern continental margin of Eurasia: evidence from the central Pontides (Turkey) and adjacent regions. *Geological Journal*, 28: 219–238

Williams, G. H. M., Turner, S. P., Pearce, J. A., Kelley,S. P. & Harris, N. B. W., 2004. Nature of the source regions for post-collisional, potassic magmatism in Southern and Northern Tibet from geochemical variations and inverse trace element modelling. *Journal of Petrology*, 45: 555–607.

Wilson, M., Neumann, E. R., Davies, G. R., Timmermann, M. J., Heeremans, M., & Larsen, B. T., 2004. Permo–Carboniferous magmatism and rifting in Europe: Introduction. In: Wilson, M., Neumann, E.-R., Davies, G. R., Timmerman, M. J., Heermans, M. J. & Larsen, B. T. (eds), *Permo–Carboniferous Magmatism and Rifting in Europe. Geological Society, Special Publications*, 223: 1–10.

Winchester, J. A. & Floyd, P. A., 1977. Geochemical discrimination of different magma series and their differentiation products using immobile elements. *Chemical Geology*, 20: 325–343.

Wolska, A., 1984. Charakterystyka petrograficzna i chemiczna diabazu z Niedźwiedziej Góry. (In Polish, English summary). *Przegląd Geologiczny*, 375: 391–396.

Zajączkowski, W. A., 1972. *Projekt badań dla wstępnego rozpoznania geologii złoża melafiru w Mękini* (In Polish, archival manuscript). Państwowy Instytut Geologiczny, Sosnowiec, 32 pp.

Żaba, J., 1995. The structural Evolution of Lower Palaeozoic Succession in the Upper Silesia Block and Małopolska Block Border Zone (Southern Poland). (In Polish, English summary). *Przegląd Geologiczny*, 43: 838–842.

Żaba, J., 1999. The structural evolution of Lower Palaeozoic succession in the Upper Silesian and Małopolska Block border zone, Southern Poland. (In Polish, English summary). *Prace Państwowego Instytutu Geologicznego*, 166: 1–162.

Żabiński, W., 1960. Z badań krzemianowo-magnezowych produktów przeobrażania melafirów krakowskich. (In Polish). *Sprawozdania z Posiedzeń Komisji Naukowych PAN, Oddział w Krakowie*: 325–326.

Żelaźniewicz, A., Pańczyk, M., Nawrocki, J. & Fanning, M., 2008. A Carboniferous/Permian, calc-alkaline, I-type granodiorite from Małopolska Block, Southern Poland: Implications from geochemical and U-Pb zircon data. *Geological Quarterly*, 52: 301–308.